ICTJA-CSIC
Lluís Solé i Sabarís S/N
08028 BARCELONA, SPAIN
e-mail: ahernandez@ictja.csic.es
armandhernandezh@gmail.com

Barcelona, 5th December 2018

Dear Editor,

Please find enclosed the revised version of the manuscript entitled "*Reconciling North Atlantic climate modes: Revised monthly indices for the East Atlantic and the Scandinavian patterns beyond the 20th century*" (essd-2018-86) and a detailed explanation of our modifications to the text and figures according to the reviewers' comments.

We hope that the new version of the manuscript would be suitable for publication in the *Earth System Science Data.*

Yours sincerely,

Dr Armand Hernández, on behalf of authors

C/ SOLÉ I SABARÍS, S/N
08028 BARCELONA SPAIN
TEL.: +34 93 409 54 10
FAX.: +34 93 411 00 12

Interactive comment on "Reconciling North Atlantic climate modes: Revised monthly indices for the East Atlantic and the Scandinavian patterns beyond the 20th century" by Laia Comas-Bru and Armand Hernández

Anonymous Referee #1

We thank the reviewer for their positive and useful comments.

Response to specific Comments:

1. A main comment would be that I find the title, and subsequent content a bit misleading in that it purports to provide monthly indices, whereas the indices in the paper are seasonal.

Thanks for highlighting something that was not clear in the manuscript. The indices that we provide are monthly indices calculated for seasonal windows (please, see the files uploaded in PANGAEA). To make this clear, we have modified Figures 3 and 4 to show the monthly indices instead of their seasonal averages. See our answer to point 2 below for further clarification.

2. A further methodological point is that it is not at all clear what is meant by "composites" throughout the paper, nor is it clear how these are constructed. I guess it is a combined index using different reanalyses, or do you mean combining monthly indices into seasonal indices? Exactly how these are combined should be made clear. I found this a bit confusing, but it should be stratightforward to clarify. Combination of time series from different reanalyses will involve splicing of some sort, and this should be explained clearly.

Indeed, the "composites" have been calculated averaging the reanalyses outputs for their overlapping periods. We have rephrased the methodology section 2.3 to clarify this point:

"Composite series of the NAO, EA and SCA patterns have been calculated for each 3-month season independently. Each individual month was given the average of the available EOF-based series with a confidence interval that corresponds to their standard deviation. The number of EOF-based series used for any given month is provided here along with the composite series. Since the EA and the SCA do not always correspond to the 2nd and 3rd EOF, respectively, a selection of what series to include in each composite based on their spatial patterns was done in advance (see Table 3 for a list of monthly EOFs included in each composite)."

We have also included an explanation sentence in the results section 3.2.1 to avoid confusions:

"Instead, since the correlations amongst datasets are very high (DJF: $\rho < 0.9$; MAM: $\rho > 0.8$; JJA: $\rho > 0.6$; SON: $\rho > 0.9$; Table S3), we have created robust composite series of each climate mode on the basis of their geographical representations as described in Table 3. This was done by averaging the overlapping EOF-based time-series that display either the NAO, EA or SCA (WA for MAM)."

Response to minor comments:

Page 1, Line 34: I would add the recent study by Hall and Hanna, 2018, IJOC, here, to broaden the scope of the literature. This paper also finds inconsistencies in EOFs 2 and 3 for summer.

We have included this reference.

Page 2, Line 6: Other nodes are used, such as Lisbon and Gibraltar, and this should be acknowledged and referenced here.

We agree with the referee and have re-written the sentence to include the main references using Lisbon and Gibraltar.

"The NAO is commonly described by an index calculated as the difference in normalized SLP over Iceland and the Azores (Cropper et al., 2015; Rogers, 1984), Lisbon (Hurrell and van Loon, 1997) or Gibraltar (Jones et al., 1997), but there are a number of robust alternatives to this classical definition of the NAO index such as Empirical Orthogonal Function analysis (EOF; Folland et al., 2009)."

Page 2, line 22: I would be more circumspect here. Although intuitively a positive EA should equate to positive SLP anomalies in line with SCA, the CPC index is based on the reverse of this, and a number of studies take this position (Woollings et al., 2010, QJRMS; Moore et al., 2011 QJRMS; Wulff et al., 2017, GRL; Hall and Hanna, 2018, IJOC among many) so it is incorrect to promote this view of the EA as the standard one. It doesn't actually matter, the relationships are the same just inverted. It would be better to state: "Here we take the positive phase of the EA to be ….. "

We have re-written this sentence as suggested:

"Here we use the positive phase of the EA as a strong centre of positive SLP anomalies offshore Ireland."

Page 2, line 29, Again it is appropriate to cite Hall and Hanna, 2018, IJOC

Done.

Page 3, lines 15-20. It is also worth noting that EOFS are statistical constructs and are not always associated with climate physics (Dommenget and Latif, 2002, J. Climate). Also some acknowledgement that the constructed EOFs are influenced by the region selected.

We agree with the reviewer's comment and have modified this paragraph accordingly.

"… while EOF-based indices better capture the inter-annual variability in an area larger than the exact location of the centres of action (Folland et al., 2009), they are constrained by (i) the accuracy of the reanalysis products from which they are derived; (ii) the non-stationarity of the EOF pattern;(iii) the orthogonality imposed by the EOF technique; (iv) the fact that the constructed EOFs are influenced by the region selected; and (iv) having to repeat the analysis every time an update is required, which may change previously obtained time-series (Wang et al., 2014; Cropper et al., 2015).

It is also worth noting that the EOFs are statistical constructs and are not always associated with climate physics (Dommenget and Latif, 2002)"

Pages 3-4 Data section. Were timeseries of station and gridded data assessed and corrected for any inhomogeneities which could arise through artificial means such as changing instrumentation, changes in density of records, etc?

Datasets were already tested for inhomogeneities by their corresponding sources: Klein Tank et al. 2002 and MetEireann. We have noted this in the manuscript, where the instrumental data is introduced:

"Datasets were tested for inhomogeneities already by their sources (Table 1)."

For transparency, we have added another supplementary table with the details of all the meteorological stations that were considered, as well as a paragraph in the manuscript to explain the selection procedure:

"A set of meteorological stations were selected according to their proximity to the EA and SCA centres of action shown in our EOF analyses: Ireland for the EA and Norway for the SCA. Only one meteorological station with SLP measurements in Ireland could be used in this study: Valentia Observatory. On the other hand, five Norwegian stations with SLP data were located in the region of interest. The most suitable Norwegian station was further selected according to three criteria: i) length of the record, ii) continuity (i.e. the least missing data, the better) and iii) correlation with the EOF-based SCA time-series. Bergen Florida (Norway) was the station which better fulfilled these criteria. Details of all meteorological stations are available in Table S1."

Page 4, line 14. It is misleading to state that the common definition of a positive EA is positive SLP anomalies, in view of the comment and references above. Change to something like "our definitions"

We have followed the referee's suggestion.

"The polarities of the derived EOF time-series have been fixed to correspond to our definitions of the EA and the SCA (see section 1), which coincide with positive centres of action over the Atlantic and Scandinavia, respectively (Figs. 1 and S1-S4)."

Page 4, Line 32. How are the years of the moving windows defined, in reference to the window (start, end, centred-which is not possible with a 30 year window)?

Each time window is defined from *i* to *i+30*, where *i* is the oldest year of overlap between the time-series. We have added this text in the methodology section 2.4.

Page 6, Line 31: Are the composites monthly? They look seasonal to me. It is unclear from the text how the composites are produced. This needs to be explained clearly. This section is unclear, with confusing terminology about monthly time series when the figures show seasonal time series.

Following the first two general comments, we revised this section to avoid misunderstandings. Please see our answers to those comments above.

Page 8. Line 6. What is the 10-year filter? Is it a simple moving average, or some sort of Gaussian filter? The caption just says "bandpass" Can you be more specific?

We have included a brief explanation in the methodology section.

"Decadal variability of the time-series (Section 3.2.3) has been explored after filtering the time-series with a 2nd order low-pass Butterworth filter with a cut-off frequency of 1/10 (as implemented in the "butter" function of Matlab© R2018a)."

Page 8, lines 9-10 "...until a decrease towards a minimum starts in c. 1920" It is not clear what is meant by this as from the figure the minimum appears to be reached in 1920.

This point is addressed in the next comment, where we show the revised text.

Page 8, lines 11-14: I don't find these descriptions particularly convincing when looking at the figure

We agree with the reviewer that this text was not convincing, nor it was clear to the reader. The revised text reads as follows:

"Figures 3 and 4 show that most variability in EA_{comp} and SCA_{comp} is observed at inter-annual scales but some decadal variability is also evident in Figure 6. Overall, all 10-yr filtered indices fluctuate around the zero-line with no evident trend, except for one period when both series are persistently positive: during winter at the end of the 19th century (Fig. 6a). During this season, both indices show similar trends between 1880 and 1920, when a decoupling occurs. In addition, the SCA experiences a large change of sign during the first three decades of the 20th century. Focusing on spring, we observe different patterns for both the EA and the WA with an EA absolute maximum at c. 1915 and two SCA minima at c.1930 and c.1960."

Page 8 line 15-16. I am highly sceptical about the reality of the first 20 years or so of the summer SCA figure, with its extreme maxima and minima. I think this is likely to be an artefact of data quality, See ESRL web pages https://www.esrl.noaa.gov/psd/data/gridded/20thC_ReanV2c/opportunities.html There is some evidence of this in Figure 6 panel b) as well.

We thank the reviewer for this information. To highlight the need to be cautious on this section of the data, we have highlighted it in all our figures with a grey band and have also modified the text to make this point clear:

"The extreme absolute minima at the start of the summer SCA_{comp} record (Fig. 4) seems to result from a low-pressure bias in marine records (Woodruff et al., 2005, Wallbrink et al., 2009) that has affected 20CRv2c fields such as the sea-level pressure from 1851 to c. 1865 (further information on this can be found here https://www.esrl.noaa.gov/psd/data/gridded/20thC_ReanV2c/opportunities). Since the 20CRv2c is the only reanalyses dataset covering that early period, we cannot provide an alternative. Instead, this period of low-confidence has been highlighted in all our figures with a grey band."

Responses to technical corrections

Page 1 line31: remove comma after "attention"

Done.

Page 5 line 29: should it be DJF: p>0.9?

Perhaps we do not understand the referee's suggestion but we believe the text in Page 5 line 29 is correct.

Interactive comment on "Reconciling North Atlantic climate modes: Revised monthly indices for the East Atlantic and the Scandinavian patterns beyond the 20th century" by Laia Comas-Bru and Armand Hernández

Anonymous Referee #2

We thank the reviewer for their comments.

Respose to general comments

1. Since the controlling mechanisms of the EA and the SCA are mentioned in the abstract, I would like to see a more careful description of the influence of these two patterns on climate variables and their physical meaning. Moreover, given the discrepancies across datasets and the lower percentage of variance explained by the patterns outside of the winter months, discussing their relevance would be appropriate.

We do not want to go into much detail on the influence of these two patterns on climate variables (this would be worth another manuscript!). However, we acknowledge that some indication on what these influences are would strengthen the manuscript.

Therefore, to follow the referee's suggestion and to indicate the observed impacts on the main climate variables, we have now included a new section (section 3.4 Climate impact of the composite EA and SCA series) along with a new Figure 8. These show the correlations between the new monthly EA and SCA indices with precipitation amount and surface air temperature in Europe (where the correlations are expected to be more robust).

The new section reads as follows:

"Figure 8 illustrates the monthly correlation distribution maps between our composite-series (EA$_{comp}$ and SCA$_{comp}$) versus surface air temperature and precipitation amount for the four seasons (DJF, MAM, JJA and SON) between 1901 and 2016 using the CRU-TS.4.01 dataset (Harris et al. 2014). The strongest correlations are found in winter, when these patterns are more prominent, and are consistent with previous studies (Moore et al, 2011; Comas-Bru and McDermott, 2014; Lim, 2015).

The only European regions for which the EA impacts on precipitation are strong and robust (i.e. on the same direction) throughout the year are the UK and Ireland. The predominantly weak correlations observed in other regions, far from the main centres of action, could arise from the low percentages of variability explained by each EOF pattern (<20% for EA; Table S22). Nevertheless, consistent patterns are observed in terms of precipitation amount across all seasons except in EA$_{comp}$/JJA, which also shows an anomalous relationship with temperature. We interpret this to be caused by the northerly shift of the EA centre of action in JJA (i.e. between Scotland and Iceland instead of off-shore Ireland; see Table 3 and Figures S3 and S4), that hampers its influence on the western Mediterranean region, which in turn becomes wetter with positive EA modes. Regarding the impact of the SCA on precipitation, a similar pattern with negative correlations in northern Europe and predominantly positive correlations in the circum-Mediterranean region, is observed across seasons, albeit with different strengths.

We observe a strong seasonality on the impact of both climate modes on surface air temperature. Weak correlations are found for the all seasons except JJA for the EA with non-significant correlations across all Europe in SON. The opposite is observed for SCA,

where the strongest impact on air temperature is shown in DJF (predominantly negative) and SON (predominantly positive).

Due to the low variance explained by both climate modes, they are not expected to imprint a very strong signal on the climate and thus the extent to which these correlations would be reflected in the absolute precipitation and temperature values will primarily depend on the concomitant state of the NAO, the main driver of climate variability in the region (Hurrell and van Loon, 1997; Hurrell and Deser, 2010). In addition, the impact of these atmospheric modes on the climate is not robust throughout the year. For example, none of the datasets used in this study showed a SCA pattern within the three leading EOFs in spring.

Individual EOFs such as the EA and the SCA are statistical constructs that do not necessarily represent a physically independent phenomenon linked (i.e. correlated) to climate variables in a robust manner. Full characterisation of the regional atmospheric dynamics therefore requires multiple EOFs to be taken into account (Roundy, 2015). To thoroughly characterise the climate in the region, the impacts of the EA/SCA should be investigated in conjunction with the NAO (Moore et al., 2011; Comas-Bru and McDermott, 2014; Hall and Hanna, 2018) but this is outside the scope of this study. As far as we are aware, such investigation does not exist outside the winter months."

2. The main contribution of this paper is, in my opinion, the introduction of the new, instrumental indices that date back longer than previously available ones and that have been proven consistent across different datasets. The correlation of the winter SCA with the Bergen station data is remarkably good. For this reason, I think it would be interesting to know more about the instrumental data, and mention which other stations were considered and why they were discarded.

We agree with the reviewer's comments. A new paragraph introducing the selection criteria and the stations that we were considering has been added in section 2.1. In addition, we have listed the details of all these meteorological stations in a new supplementary table (S1).

"A set of meteorological stations were selected according to their proximity to the EA and SCA centres of action shown in our EOF analyses: Ireland for the EA and Norway for the SCA. Only one meteorological station with SLP measurements in Ireland could be used in this study: Valentia Observatory. On the other hand, five Norwegian stations with SLP data were located in the region of interest. The most suitable Norwegian station was further selected according to three criteria: i) length of the record, ii) continuity (i.e. the least missing data, the better) and iii) correlation with the EOF-based SCA time-series. Bergen Florida (Norway) was the station which better fulfilled these criteria. Details of all meteorological stations are available in Table S1."

Response to specific comments

Page 1, Line 25: "The spatial structure of climate changes..." I would suggest talking about regional climate variability rather than 'climate changes', given the data span no longer than two hundred years.

Done: "The spatial structure of regional climate variability follows recurrent patterns often referred to as modes of climate variability or teleconnections, which provide a simplified description of the climate system (Trenberth and Jones, 2007)."

Page 2, Line 21: A strong centre of positive SLP anomalies is said here to be associated with above-average temperature and wetter conditions in Northern Europe. Please review this. Is it possible that those effects correspond to the positive phase of the reverse EA index, as used in other publications? (i.e., Moore et al., 2011)

Indeed! We have rephrased the sentence to match the direction of our EA index.

"Here we use the positive phase of the EA as a strong centre of positive SLP anomalies offshore Ireland. This is associated with below-average surface temperatures in Southern Europe, drier conditions over Western Europe and wetter conditions across much of Eastern Europe and the Norwegian coast (Moore et al., 2011; Rodríguez-Puebla and Nieto, 2010)."

Page 3, Line 18: The orthogonality imposed by the EOF technique should be one of the constraints listed

Agreed. We have now added this as one of the constrains:

"... while EOF-based indices better capture the inter-annual variability in an area larger than the exact location of the centres of action (Folland et al., 2009), they are constrained by (i) the accuracy of the reanalysis products from which they are derived; (ii) the non-stationarity of the EOF pattern;(iii) the orthogonality imposed by the EOF technique; (iv) the fact that the constructed EOFs are influenced by the region selected; and (iv) having to repeat the analysis every time an update is required, which may change previously obtained time-series (Wang et al., 2014; Cropper et al., 2015). It is also worth noting that the EOFs are statistical constructs and are not always associated with climate physics (Dommenget and Latif, 2002)"

Page 5, Line 6: Looking at Table 3, no discrepancies are observed across datasets for EOF 3 during MAM months

The referee is right. We have removed this from the text.

"For example, while the geographical patterns are very stable across datasets during winter (Table 3), some discrepancies are observed during summer (JJA; see EOF2 or EOF3)."

Page 5, Line 21: "Because of this spatial pattern, ..." I suggest rephrasing the sentence since the meaning is not entirely clear to me.

We have rephrased the sentence and hope it is now clearer:

"Due to the spatial extent of the winter's EOF3 positive centre of anomalies covering from Scandinavia to SW Ireland, Val$_{SLP}$ (purple dot in Figure 1 and S1-S4) is unsurprisingly correlated with all winter EOF3s ($0.5<\rho<0.6$; Table 4)."

Page 6, Line 27: I think it is erroneous to assume that the datasets have to capture the climate modes, since the variability is in the SLP data themselves. Comparing different reanalysis datasets is out of the scope of this paper, but an indication of known quality issues that might account for the differences would be suitable

Following reviewer's 1 comment, we have now added some information on the anomalous SLP observed in the 20CRv2c dataset for the period 1951-1965. This has also been highlighted in all figures with a grey box.

In order to address the reviewer's concern, we now direct the reader to Fujiwara et al., 2017, which provides an extensive review of the quality of all the reanalyses products used in this study. We've also added a short paragraph highlighting the main differences of each of the reanalyses datasets used in this study.

"Five reanalyses datasets have been used in this study (Table 2). ERA-40 (Uppala et al., 2005) is a conventional-input reanalysis used in many studies that require long-term atmospheric data. ERA-Interim (Dee et al., 2011) improves ERA-40 in that it assimilates a more complete set of observations and therefore it achieves more realistic representations of the hydrologic cycle and the stratospheric circulation relative to ERA-40, as well as it improves the consistency of the reanalysis products over time. ERA-20C (Poli et al., 2016) directly assimilates surface pressure and surface wind observations, enabling it to extend back in time to cover the entire 20th century. 20CRv2c (Compo et al., 2011) is also a surface-input reanalysis with a different assimilation procedure than that of ERA-20C. The main limitation of 20CRv2c is that it does not correct for biases in surface pressure observations from ships and buoys, which results in the anomalous SLP observed for the period 1850-1865. Finally, the NCEP/NCAR (Kalnay et al., 1996) was the first modern reanalysis of extended temporal coverage (1948 to present) and it is still widely used. For an extensive review on the quality of these datasets, the reader is referred to Fujiwara et al., 2017."

Figure 2: many data are shown on the same plot, so that it is a bit difficult to visually recognise the agreement between the series. Also, could the x axis show dates rather than number of months?

Done.

Figure 6: I suggest including DJF, MAM, JJA and SON instead of a, b, c and d on the top left corner of each panel, both for clarity and for consistency with Figures 3 and 4

Done.

Reconciling North Atlantic climate modes: Revised monthly indices for the East Atlantic and the Scandinavian patterns beyond the 20th century

5   Laia Comas-Bru[1,2], Armand Hernández[32*]

[1] UCD School of Earth Sciences. University College Dublin. Belfield. Dublin 4. Ireland.
[2] Institute of Earth Sciences Jaume Almera, ICTJA, CSIC, 08028 Barcelona, Spain

10   *Correspondence to*: Armand Hernández (ahernandez@ictja.csic.es)

Abstract. Climate variability in the North Atlantic sector is commonly ascribed to the North Atlantic Oscillation. However, recent studies have shown that taking into account the second and third mode of variability (namely the East Atlantic – EA – and the Scandinavian – SCA – patterns) greatly improves our understanding of their
15   controlling mechanisms, as well as their impact on climate. The most commonly used EA and SCA indices span the period from 1950 to present which is too short, for example, to calibrate palaeoclimate records or assess their variability over multi-decadal scales. To tackle this, here, we create new EOF-based monthly EA and SCA indices covering the period from 1851 to present; and compare them with their equivalent instrumental indices. We also review and discuss the value of these new records and provide insights into the reasons why different sources of
20   data may give slightly different time-series. Furthermore, we demonstrate that using these patterns to explain climate variability beyond the winter season needs to be done carefully due to their non-stationary behaviour. The datasets are available at https://doi.org/10.1594/PANGAEA.892769.

1 Introduction

The spatial structure of regional climate variabilityclimate changes follows recurrent patterns often
25   referred to as modes of climate variability or teleconnections, which provide a simplified description of the climate system (Trenberth and Jones, 2007). For example, a considerable fraction of inter-annual climate variability in the Northern Hemisphere is often ascribed to the North Atlantic Oscillation (NAO), which represents the principal mode of winter climate variability across much of the North Atlantic sector (Hurrell, 1995; Wanner et al., 2001; Hurrell and Deser, 2010) and explains c. 40% of the winter sea-level pressure (SLP) variability in the region (Pinto
30   and Raible, 2012). However, considering other modes of variability that have historically received less attention, better explains the overall regional SLP and climate variability. In particular, the East Atlantic (EA) and the Scandinavian (SCA) patterns have been demonstrated to significantly influence the winter European climate (Comas-Bru and McDermott, 2014; Hall and Hanna, 2018) as well as the sensitivity of climate variables such as temperature and precipitation to the NAO. Furthermore, the interplay of these modes exerts a strong impact on
35   climates at different spatio-temporal scales and have important ecological and societal impacts (e.g., Jerez and Trigo, 2013; Bastos et al., 2016) as well as impacts on the availability of, for example, wind-energy resources (Zubiate et al., 2017).

In particular, the NAO consists of a N-S dipole of SLP anomalies resulting from the co-occurrence of the Azores High and the Icelandic Low (Hurrell and VanLoon, 1997Hurrell, 1995) and modulates the extra-

1

tropical zonal flow. Its varying strength is indicated by swings between positive and negative phases that produce large changes in surface air temperature, winds, storminess and precipitation across Eurasia, North Africa, Greenland and North America (Hurrell and Deser, 2010). The NAO is commonly described by an index calculated as the difference in normalized SLP over Iceland and the Azores (Cropper et al., 2015; Rogers, 1984),), Lisbon (Hurrell and van Loon, 1997) or Gibraltar (Jones et al., 1997), but there are a number of robust alternatives to this classical definition of the NAO index such as Empirical Orthogonal Function analysis (EOF; Folland et al., 2009).

The second mode of climate variability in the North Atlantic region, the EA pattern, was originally identified in the EOF analysis of Barnston and Livezey (1987) and the exact representation of its EOF loadings is still a matter of debate. Some authors describe the EA as a N-S dipole of anomaly centres spanning the North Atlantic from East to West (Bastos et al. 2016; Chafik et al. 2017) while others characterise it as a well-defined SLP monopole south of Iceland and west of Ireland, near 52.5°N, 22.5°W (Josey and Marsh, 2005; Moore and Renfrew, 2012; Comas-Bru and McDermott, 2014; Zubiate et al., 2017). However, regardless of its exact spatial structure, the location of its main centre of action is, in all cases, along the nodal line of the NAO; often implying a "southward shifted NAO" with the corresponding North Atlantic storm track and jet stream also shifted towards lower latitudes (Woollings et al., 2010). The most common methods to obtain an index for the EA are EOF analyses (Barnston and Livezey, 1987; Comas-Bru and McDermott, 2014 Moore et al., 2013) or Rotated Principal Component Analysis (CPC, 2012), but the SLP instrumental series from Valentia Observatory, Ireland (51.93°N 10.23°W) has also been used in a limited number of studies (Comas-Bru et al., 2016; Moore and Renfrew, 2012). Here we use tThe positive phase of the EA as a(i.e. strong centre of positive SLP anomalies offshore Ireland), is associated with above-average surface temperatures in Europe, and with below-average temperatures over North America. It is also associated with wetter conditions over northern Europe and Scandinavia, and drier conditions across southern Europe (Moore et al., 2011; Rodríguez-Puebla and Nieto, 2010). . This is associated with below-average surface temperatures in Southern Europe, drier conditions over Western Europe and wetter conditions across much of Eastern Europe and the Norwegian coast (Moore et al., 2011; Rodríguez-Puebla and Nieto, 2010).

The SCA pattern is usually defined as the third leading mode of winter SLP variability in the European region and is equivalent to the Eurasia-1 pattern described by Barnston and Livezey (1987). It shows a vigorous centre at 60-70°N 25-50E with some studies showing a more diffuse centre of opposite sign south of Greenland. As far as we are aware, only EOF analyses (Comas-Bru and McDermott, 2014; Crasemann et al., 2017; Moore et al., 2013; Hall and Hanna, 2018) and Rotated Principal Component Analysis (Bueh and Nakamura, 2007; CPC, 2012) have been used to obtain a temporal index of the SCA. The positive phase of the SCA is related to a higher than average pressure anomalies over Fennoscandia, Western Russia and in some cases Northern Europe, which may lead to a blocking situation that results in winter dry conditions over the Scandinavian region, below-average temperatures across central Russia and Western Europe and wet conditions in Southern Europe (CPC, 2012; Bueh and Nakamura, 2007; Crasemann et al., 2017; Scherrer et al., 2005).

To the best of our knowledge, while NAO indices are available from a wide variety of sources such as the Climate Prediction Center, CPC-NOAA (http://www.cpc.ncep.noaa.gov); the Climate Data Guide (https://climatedataguide.ucar.edu); and the Climate Research Unit, University of East Anglia, CRU-UEA (http://www.cru.uea.ac.uk), only the CPC-NOAA provides EA and SCA indices and, in both cases, they only cover the period since 1950. Along the same lines, the NOAA-CIRE (https://www.esrl.noaa.gov/psd/data/20thC_Rean/timeseries/) provides a set of climate indices created with the

20CRv2c dataset (Compo et al., 2011), but the EA and the SCA are not included. This urges scientists willing to use a longer EA and/or SCA index to do their own EOF analyses, thereby increasing the likelihood that different studies will use EOF-based EA and SCA indices that may be based on a different geographical area (i.e., North Atlantic versus Northern Hemisphere), months (i.e., winter versus annual) or time-periods, while at the same time

5   increasing the likelihood of computational discrepancies. Therefore, making long monthly EOF-based indices of the EA and SCA readily available will probably contribute to an increased consistency across research studies such as those that aim at calibrating proxy-based records of past climate variability.

On the other hand, station-based indices have the advantage of providing continuous records that may extend back beyond the 20th Century, when reanalysis data are more scarce (Cropper et al., 2015). However, the

10   main compromises of such methodology are that (i) using station-based indices implies a fixed location of the mode's centres of action; even though non-stationarities in the geographical location of such centres, in particular those of the NAO, have been widely demonstrated (Blade et al., 2012; Lehner et al., 2012); (ii) the SLP recorded by meteorological stations may not be regionally representative due to local biases (i.e. artificial changes in their local environments; Pielke et al., 2007); and (iii) early SLP recordings may be compromised by the use of less

15   reliable old instrumental devices (Aguilar et al., 2003; Trewin, 2010). By contrast, while EOF-based indices better capture the inter-annual variability in an area larger than the exact location of the centres of action (Folland et al., 2009), they are constrained by (i) the accuracy of the reanalysis products from which they are derived;, (ii) the non-stationarity of the EOF pattern; and (iii) the orthogonality imposed by the EOF technique; (iv) the fact that the constructed EOFs are influenced by the region selected; and (iv) having to repeat the analysis every time an

20   update is required, which may change previously obtained time-series (Wang et al., 2014; Cropper et al., 2015). It is also worth noting that the EOFs are statistical constructs and are not always associated with climate physics (Dommenget and Latif, 2002). (i) the accuracy of the reanalysis products from which they are derived, (ii) the non-stationarity of the EOF pattern and (iii) having to repeat the analysis every time an update is required, which may change previously obtained time series (Comas Bru and McDermott, 2014; Wang et al., 2014; Cropper et

25   al., 2015).

Here, we present a compilation of monthly indices of the EA and the SCA based on meteorological stations and from five reanalyses products. The instrumental series go back to 1866 and 1901, respectively, while the EOF-based series go back to 1851. To the best of our knowledge, these are the longest EA and SCA datasets made available to the scientific community. We also provide a comprehensive comparison of the instrumental and

30   EOF-based indices, including their ability to capture seasonal changes of the SLP field in the region.

2 Data and Methods

2.1 Instrumental data

A set of meteorological stations were selected according to their proximity to the EA and SCA centres of action shown in our EOF analyses: Ireland for the EA and Norway for the SCA. Only one meteorological

35   station with SLP measurements in Ireland could be used in this study: Valentia Observatory. On the other hand, five Norwegian stations with SLP data were located in the region of interest. The most suitable Norwegian station was further selected according to three criteria: i) length of the record, ii) continuity (i.e. the least missing data,

the better) and iii) correlation with the EOF-based SCA time-series. Bergen Florida (Norway) was the station which better fulfilled these criteria. Details of all meteorological stations are available in Table S1.

Thus, dDaily records from Valentia Observatory (Ireland; 01/10/1939-31/12/2016) and Bergen Florida (Norway; 01/01/1901-31/10/2016) as well as monthly data from Valentia Observatory (January 1866 to December 2013; Table 1) have been used to calculate the monthly series that form our instrumental indices. Only one day (14/11/2012) and four months (December 1938; May 1872, 1873 and 1874) were missing from the Valentia SLP data. Filling the gap in the daily time-series with its long-term average does not improve the accuracy of the corresponding monthly mean, and so this day has been omitted in the calculations. Datasets were tested for inhomogeneities already by their sources (Table 1). A long continuous record of monthly SLP for Valentia was obtained by merging the monthly averages from January 1866 to December 2016 and the computed monthly means for the period since November 1939 on the basis that the overlapping period (1939-2013) showed a correlation $\rho > 0.99$. Hereafter, standardised monthly SLP anomalies for these stations are named Val_{SLP} and Ber_{SLP}.

2.2 Empirical Orthogonal Function (EOF) analysis ~~Gridded datasets~~

Five reanalyses datasets have been used in this study (Table 2). ERA-40 (Uppala et al., 2005) is a conventional-input reanalysis used in many studies that require long-term atmospheric data. ERA-Interim (Dee et al., 2011) improves ERA-40 in that it assimilates a more complete set of observations and therefore achieves more realistic representations of the hydrologic cycle and the stratospheric circulation relative to ERA-40, as well as it improves the consistency of the reanalysis products over time. ERA-20C (Poli et al., 2016) directly assimilates surface pressure and surface wind observations, enabling it to extend back in time to cover the entire 20th century. 20CRv2c (Compo et al., 2011) is also a surface-input reanalysis with a different assimilation procedure than that of ERA-20C. The main limitation of 20CRv2c is that it does not correct for biases in surface pressure observations from ships and buoys, which results in the anomalous SLP observed for the period 1850-1865. Finally, the NCEP/NCAR (Kalnay et al., 1996) was the first modern reanalysis of extended temporal coverage (1948 to present) and it is still widely used. For an extensive review on the quality of these datasets, the reader is referred to Fujiwara et al., 2017.

Empirical Orthogonal Function (EOF) analysis was performed on the above-mentioned five reanalyses datasets of monthly SLP for a constrained Atlantic sector (100°W-40°E, 10-80°N; Table 2) using the *pca* function of Matlab© R2018a. As in previous studies, the SLP anomalies were geographically equalized prior to the analyses by multiplying them by the square root of the cosine of its corresponding latitude (North et al., 1982). The percentage of variance explained by each EOF is shown in Table S2.

To maximise the representation of each pattern across seasons, and because the relative strength of the three main modes of variability is not constant throughout the year, all EOFs have been calculated for each three-month season (DJF, MAM, JJA and SON). Although we only used SLP fields, these patterns are also recognisable if using different levels of the atmosphere. See Wallace and Gutzler (1981) and Cradden and McDermott (2018) for patterns using 500-mb heights and Barnston and Livezey (1987) for 700-mb heights.

The polarities of the derived EOF time-series have been fixed to correspond to ~~the common~~our definitions of the EA and the SCA (see section 1), which coincide with positive centres of action ~~over~~ offshore Ireland and over ~~the Atlantic and~~ Scandinavia, respectively (Figs. 1 and S1-S4). This is consistent with the

4

expected climate patterns and in the case of the EA, is compatible with the usage of SLP data from Valentia Observatory (Ireland) as an instrumental EA index (Comas-Bru et al., 2016; Moore and Renfrew, 2012; see section 3.1).

2.3 ~~Correlations~~ **Composite time-series**

Monthly c~~C~~omposite series of the NAO, EA and SCA patterns~~both climate modes~~ have been calculated for each 3-month season independently. Each individual month was given the average of the available EOF-based series with a confidence interval that corresponds to their standard deviation. The number of EOF-based series used for any given month is provided here along with the composite series.~~3-month season as the average of the EOF-based series at any given year with a confidence interval that corresponds to their standard deviation~~. ~~However, s~~Since the EA and the SCA do not always correspond to the 2nd and 3rd EOF, respectively, a selection of what series to include in each composite based on their spatial patterns was done in advance (see Table 3 for a list of individual EOFs included in each composite).

2.4 Data analysis

2.3 Correlations

All correlations have been computed using Spearman rank coefficients (rho, ρ) to avoid assumptions about normally distributed data that are inherent in some other correlation coefficients. The Spearman rank correlation coefficient is generally expressed as Eq. (1):

$$\rho = 1 - \frac{6\sum_{i=1}^{n} d_i^2}{n(n^2-1)} \tag{1}$$

Where n is the number of measurements in each of the two variables in the correlation and d_i is the difference between the ranks of the ith observation of the two variables.

When computing the 30-year running correlations, the significance of the correlations for each time window was done using a Monte Carlo approach ~~and~~ following the methodology described in Ebisuzaki (1997). Each time window is defined from i to $i+30$, where i is the oldest year of overlap between the time-series.

Decadal variability of the time-series (Section 3.2.3) has been explored after filtering the time-series with a 2nd order low-pass Butterworth filter with a cut-off frequency of 1/10 (as implemented in the *butter* function of Matlab[©] R2018a).

3 Results and discussion

3.1 Instrumental vs EOF-based series

In order to identify the most suitable meteorological station to reconstruct each teleconnection index, we first need to investigate the robustness of their spatial structures across reanalyses datasets (Figs. 1 and S1-S4). For example, while the geographical patterns are very stable across datasets during winter (Table 3), some discrepancies are observed during ~~seasons like spring (MAM; see EOF3 in Table 3) or~~ summer (JJA; see EOF2 or EOF3).

Moore and Renfrew (2012) used SLP data from Valentia Island (Ireland; Table 1) to derive an EA station-based index and, even though this meteorological station is not located at EA centre of SLP anomalies, the correlation coefficients between its winter values (when the mode is strongest) and EOF2 are very high ($0.7 < \rho < 0.9$; Fig. 2a; Table 4). Furthermore, our results show that when an EA pattern is identified in the reanalysis products,

5 the location of Valentia Observatory lies within the main area of SLP anomalies. For an example, see the relative location of the purple dot and the yellow centre of anomalies of EOF2 in Figure 1. This indicates the suitability of using Valentia Observatory data as a proxy of EA variability.

After an exhaustive investigation to find a long and continuous instrumental SLP dataset in Fennoscandia as a measurement of the strength of the Scandinavian pattern, we suggest using the SLP record from Bergen

10 Florida (Norway; Table 1), which falls on the SCA's centre of action as shown by the pink dots in Fig 1. This decision is further supported by the high resemblance between this meteorological dataset and the third EOF of the winter SLP field ($0.7 < \rho < 0.8$; Fig. 2b; Table 4). This EOF3 corresponds to the SCA pattern defined by Barnston and Livezey (1987) extended towards Ireland and UK and, in some cases, most of Northern Europe (ERA-20C, ERA-40, ERA-interim and NCEP/NCAR; see Figs. 1 and S1-S4). <u>Due to the spatial extent of the winter's EOF3</u>

15 <u>positive centre of anomalies covering from Scandinavia to SW Ireland, Val$_{SLP}$ (purple dot in Figure 1 and S1-S4)</u> ~~Because of this spatial pattern, Val$_{SLP}$~~ is unsurprisingly correlated with all winter EOF3s ($0.5 < \rho < 0.6$; Table 4).

Consistent with previous studies (e.g., Hurrell et al., 20~~1~~0~~3~~; Moore et al., 2013) EOF1 represents the NAO across seasons and datasets, albeit with slight changes in the extension and/or intensity of its southern pole (Figs. 1 and S1-S4). However, EOF2 and EOF3 are far from showing a homogeneous pattern over the course of

20 the four seasons and across the five reanalysis datasets.

During spring, the spatial structure of the EA (Figs. 1 and S1-S4) is recognised in EOF3. This is consistent with the moderate to high correlations between EOF3 and Val$_{SLP}$ ($0.6 < \rho < 0.7$; Table 4). However, due to the observed (in some cases weak) negative pole over Scandinavia, Ber$_{SLP}$ is poorly correlated to EOF3 ($-0.4 < \rho < -0.1$; Table 4). As the spatial patterns of EOF2 show a predominant centre over the N. Atlantic Ocean (c

25 $40°N$) in all datasets, their time series are uncorrelated with our instrumental records (Figs. 1 and S1-S4, Table 4). This mode of variability is similar to the Western Atlantic (WA) pattern defined by Wallace and Gutzler (1981).

Not surprisingly, the overall picture over the course of summer is a bit more complicated than in other seasons, when most datasets are consistent. In this case, Val$_{SLP}$ shows moderate to high correlations with EOF2

30 ($0.6 < \rho < 0.7$; Table 4) except for ERA-interim, for which the strongest correlations are observed with EOF1 and EOF3 ($\rho = 0.6$). However, most of these EOF2s represent an extended Scandinavian pattern (Table 4) the centre of which covers the location of Valentia Observatory, instead of the EA. A clear EA pattern is only observed for EOF3 ERA-20C and a northwardly shifted EA pattern is found in EOF2 ERA-interim and EOF3 NCEP/NCAR (Table 3). These discrepancies between ERA-interim and the other datasets arise because (i) EOF1 depicts a NAO

35 pattern with a southern pole shifted towards Northern Europe; (ii) EOF2 represents a pattern similar to a northwardly shifted EA; and (iii) EOF3 is equivalent to the extended SCA pattern also found in winter across all datasets (see Figs. 1 and S1-S4).

Correlations between summer Ber$_{SLP}$ and EOF3 are moderate to high only for 20CRv2c and ERA-40 ($\rho > 0.6$; Table 4) because they represent the classical SCA pattern; with a centre of anomalies only over

40 Fennoscandia and the North Sea. However, as a result of this spatial pattern, moderate correlations are also found

6

with EOF2 across datasets (0.5<ρ<0.7; except ERA-interim). Regarding ERA-interim's EOF2, the weak correlation with Ber_{SLP} (ρ=0.3) is due to the EA having migrated northwards. In contrast with the rest of the seasons, and as previously noted for Val_{SLP}, a range of moderate to high correlations are observed between summer EOF1 and Ber_{SLP} as a result of the observed "summer NAO" pattern already defined in previous studies (Blade et al., 2012; Folland et al., 2009).

In the case of autumn, a more coherent picture across datasets is observed: EOF1 represents a NAO with a weak southern pole that, in some cases, migrates towards Europe; EOF2 is equivalent to the EA with a weak negative pole over Scandinavia; and EOF3 shows a SCA pattern similar to the one obtained for the winter months. Consequently, Val_{SLP} is correlated with EOF2 (0.6<ρ<0.7) and Ber_{SLP} to the EOF3 (0.6<ρ<0.8) for all the reanalysis products. However, due to the extended SCA in EOF3, Val_{SLP} is also moderately correlated to it for all datasets except ERA-interim, where Valentia Observatory lies at the edge of the centre. In addition, Val_{SLP} is also moderately correlated with ERA-interim's EOF1 as a result of the NAO's southern pole being shifted towards NW Europe (Fig. S3).

In summary, it has been shown that winter and autumn Val_{SLP} and Ber_{SLP} indices correlate with EOF2 and EOF3, respectively. In contrast, the summer EA and SCA patterns swap their order in some datasets but good correlations are found when the geographical representation of the EOFs is taken into account. During spring, the EA pattern is represented by EOF3 across all datasets, and EOF2 shows the WA pattern. In this case, the SCA pattern is not reflected in any of the first three components of the EOF analysis.

3.2 New monthly EA and SCA time-series

3.2.1 Monthly composites

Each reanalysis dataset has advantages and shortcomings when it comes to its ability to ~~capture~~ reproduce the different climate modes and, outlining objective indicators to select the reanalysis dataset that performs best is outside of the scope of this study. Instead, since the correlations amongst datasets are very high (DJF: ρ<0.9; MAM: ρ>0.8; JJA: ρ>0.6; SON: ρ >0.9; Table ~~S1~~S3), we have created robust composite series of each climate mode on the basis of the~~ir~~ geographical representations as described in Table 3. This was done by averaging the overlapping EOF-based time-series that display either the NAO, EA or SCA (WA for MAM). See section 2.2 for further details. ~~Thus, monthly time series, with confidence intervals, have been constructed with the EOFs that display either the NAO, EA or SCA (WA for MAM).~~

Figures 3 and 4 show the monthly time-series of EA_{comp}/SCA_{comp}, Val_{SLP}/Ber_{SLP} and EA_{cpc}/SCA_{cpc} (the longest available records from CPC, 2012). Spearman rank coefficients between these series are in Tables 5 and 6. For winter, Val_{SLP} is robustly correlated with EA_{comp} (ρ=0.8) and moderately correlated with SCA_{comp} (ρ=0.5; Table 5). This results from the fact that the datasets forming SCA_{comp} all show an "extended SCA" pattern (which covers UK and Ireland, and therefore Valentia Observatory; see Figs 1 and S1-S4). On the other hand, Ber_{SLP} exhibits a very high correlation (ρ=0.8) with SCA_{comp} and is uncorrelated with EA_{comp}, even though all EA spatial patterns show a weak secondary pole of negative SLP anomalies over Scandinavia (Figs. 1 and S1-S4). It seems therefore that only the main centre of action is reflected in the correlations (Table 5).

With regard to spring, Val_{SLP} is moderately correlated with EA_{comp} (ρ=0.7) and uncorrelated with the WA_{comp} (ρ=0.1). On the other hand, Ber_{SLP} is uncorrelated with either EA_{comp} or WA index (Table 5) because

Bergen Florida lies at the edge of the SLP dipole resulting in this station being insensitive to these climate patterns (purple dot in Figs. 1 and S1-S4).

For summer, Val_{SLP} shows a low ($\rho=0.4$) and medium-to-high ($\rho=0.\underline{5}\cancel{6}$) correlation with EA_{comp} and SCA_{comp}, respectively. The low correlation between Val_{SLP} and EA_{comp} for this season reflects the inconsistency of the EA pattern across the different reanalysis datasets (note that the degree of correlations amongst EOFs is the lowest in summer; Table $\cancel{S1}\underline{S3}$). Consequently, only three datasets – ERA-20C, ERA-interim and NCEP/NCAR – were used to construct the summer EA_{comp} (Table 3) with the last two showing a clear northern migration of its anomaly centre that leaves Valentia Observatory outside the area sensitive to this pattern (pink dot in Figs. S3 and S4). By contrast, the observed relatively high correlation between Val_{SLP} and SCA_{comp} is due to the extended SCA (Figs. 1 and S1-S4). Regarding Ber_{SLP}, this is poorly correlated with EA_{comp} ($\rho=0.2$) and moderately correlated with SCA_{comp} ($\rho=0.6$; Table 5) as a result of the robust "extended SCA" patterns used to create SCA_{comp} (Table 3).

As far as autumn is concerned, Val_{SLP} displays similar moderate correlations with EA_{comp} and SCA_{comp} ($\rho=0.5$), again as a result of the similarity between the EA and the "extended SCA" patterns. Moreover, Ber_{SLP} is negatively correlated with EA_{comp} ($\rho=-0.2$) because of the negative secondary pole of the EA (see Figs 1 and S1-S4), and highly correlated with SCA_{comp} ($\rho=0.7$).

3.2.2 Consistency of the correlations

To assess the temporal stability of the correlations discussed above, we have calculated 30-yr moving correlations between EA_{comp}/SCA_{comp} and Val_{SLP}/Ber_{SLP}. As evident in Figure 5, these relationships are only stationary (and constantly significant at $\rho > 0.7$) during winter, when the two atmospheric climate modes are more robustly expressed. During spring, correlations between EA_{comp} and Val_{SLP} vary across a large range of values: from non-significant correlations during 1880's, early and mid-20th century (ca. 1950-1965) to moderate-to-high correlations ($\rho>0.6$) during 1930's and 1990's. By contrast, the correlations between SCA_{comp} and Ber_{SLP} are non-significant for almost the entire time interval (1901-2016), with only two small windows – between ca. 1925 and 1935 and around 1970 – exhibiting significant correlations ($\rho\sim0.5$). This results from the spring composite in Figure 5 representing the WA instead of the SCA. The EA correlations during summer (Fig. 5a) show the largest variability, with correlations peaking in 1940's ($\rho>0.6$) and after 1980. Non-significant correlations are found for the reminding periods. Regarding summer, SCA_{comp} and Ber_{SLP} are moderately correlated in the interval 1930-1980 and for a short period at the end of the 20th century. Autumn EA_{comp} moderately correlates with Val_{SLP} except for 1895-1920 and after ca. 1990, while SCA_{comp} is only significantly correlated with Ber_{SLP} in the period before ca. 1935 and after ca. 1965.

These results demonstrate that the station-based indices may be used as reference during the winter season but, beyond that, they ought to be used with caution due to the non-stationary behaviour of the EA and SCA patterns. For these non-winter seasons, almost opposite patterns of significance vs non-significance are found (i.e. EA_{comp} and Val_{SLP} show significant correlations when the SCA_{comp} and Ber_{SLP} correlations are not significant and vice versa). This may result from a displacement of their respective centres of action through time, similarly that what has been suggested for other climate modes of variability (i.e., NAO, AMO, ENSO and PDO) during these seasons for last two centuries in the North Atlantic sector (Hernández et al., 2016).

3.2.3 Decadal variability of new EA and SCA time-series

Figures 3 and 4 show that most variability in EA$_{comp}$ and SCA$_{comp}$ is observed at inter-annual scales but some decadal variability is also evident in Figure 6. Overall, all 10-yr filtered indices fluctuate around the zero-line with no evident trend, except for one period when both series are persistently positive: during winter at the end of the 19th century (Fig. 6a). During this season, both indices show similar trends between 1880 and 1920, when a decoupling occurs. In addition, the SCA experiences a large change of sign during the first three decades of the 20th century. Focusing on spring (Fig. 6b), we observe different patterns for both the EA and the WA with an EA absolute maximum at c. 1915 and two SCA minima at c.1930 and c.1960. The extreme absolute minima at the start of the summer SCA$_{comp}$ record (Fig. 4) seems to result from a low-pressure bias in marine records (Woodruff et al., 2005, Wallbrink et al., 2009) that has affected 20CRv2c fields such as the sea-level pressure from 1851 to c. 1865 (further information on this can be found here https://www.esrl.noaa.gov/psd/data/gridded/20thC_ReanV2c/opportunities). Since the 20CRv2c is the only reanalyses dataset covering that early period, we cannot provide an alternative. Instead, this period of low-confidence has been highlighted in all our figures with a grey band. ~~the EA experiences a large change of sign during the first three decades of the 20th century, with the SCA following a similar trend until a decrease towards a minimum starts in c. 1920. A similar trend, albeit smaller in range, is observed at the end of the 20th century and then quickly followed by a rapid decline in both, the EA and the SCA. If we now focus on spring, we will see a prolonged period (from ca. 1860 to ca. 1935) during which the EA and the WA follow opposite trends almost continuously. After that (and especially after ca. 1980) both indices follow a lagged pattern (although with different amplitudes). A more detailed investigation - outside the scope of this study - would be required to fully understand the causes of the extreme absolute minima at the start of the summer SCA$_{comp}$ record (Fig. 4). Unfortunately, only one reanalyses dataset covers that early period and perhaps its ability to capture decadal SLP variability at the end of the 19th century is limited.~~ During the rest of the period, EA$_{comp}$ and SCA$_{comp}$ alternate between similar (e.g. 1965-2000) and opposite patterns (e.g. 1910-1925), with amplitudes that gradually decrease towards present. Autumn EA$_{comp}$ and SCA$_{comp}$ alternate between in-phase (e.g. 1990-2000) and out-of-phase (e.g. 1955-1965) states.

3.3 Composites vs CPCs

To further check the performance of our composite series, we have compared them to the most widely used series from the CPC (CPC, 2012; Figs. 3 and 4; Table 6).

The NAO index from CPC (NAO$_{cpc}$) is moderately-to-very highly correlated with our NAO-composite across all seasons (Table 6; 0.6<ρ<0.8). The EA index (EA$_{cpc}$) shows a moderate negative correlation with winter EA$_{comp}$ (ρ=-0.6) and low negative correlations with the other seasons (ρ=-0.3; Table 6). These negative correlations are due to the fixed polarity of the EA pattern: the main anomaly centre of our EA is positive, while that of the CPC is negative (this can be seen contrasting the spatial patterns of their teleconnection patterns – http://www.cpc.ncep.noaa.gov/data/teledoc/ea_map.shtml for the EA and http://www.cpc.ncep.noaa.gov/data/teledoc/scand_map.shtml for the SCA – and our Figures 1 and S1-S4; Comas-Bru and McDermott (2014) provide an extensive discussion on this). These negative correlations are consistent with the correlations between EA$_{cpc}$ and Val$_{SLP}$ (Table 7) as well as the running correlations discussed below. Regarding the SCA index, SCA$_{cpc}$ exhibits a low correlation with SCA$_{comp}$ for all seasons (ρ<0.4; note that the

composite for spring is reflecting the WA pattern and hence it has not been compared with the CPC indices). The moving correlations (30-year sliding window) between the seasonal EA_{comp}/EA_{cpc} (Fig. ~~6a~~7a) and SCA_{comp}/SCA_{cpc} (Fig. ~~6b~~7b) are consistent with the correlations in Table 6. For winter and summer, the correlations between EA_{comp} and EA_{cpc} are fairly constant ($\rho<-0.5$). However, non-significant correlations are obtained for autumn during the entire time period (1950-2016) and, during spring, only the period between 1970 and 2000 is significant ($\rho<-0.4$); with the exception of few time-windows at the end of the 1980's. Regarding the temporal variability of the correlations between SCA_{comp} and SCA_{cpc}, these are only significant ($\rho>0.4$) after 1990 for the winter season (Fig. 5b).

Overall, these results suggest that the difference in methodology between our EOFs and the one followed by the CPC, and/or the difference in the reanalysis products used is not relevant for the NAO, but it becomes critical for the EOFs that account for a smaller percentage of the total SLP variance ($>30\%$ vs $10-20\%$; Table S2). The low correlations observed beyond the winter season could be linked to a non-stationary behaviour of the EA and SCA resulting in migrations of their centres that are not adequately captured by our methodology and/or that employed by the CPC, or in the reanalyses products from which the indices are derived.

This is further supported by the geographical displays of seasonal EA_{cpc} and SCA_{cpc} (see URLs above). The EA_{cpc} consists of a dipole with negative anomalies that spans from the central North Atlantic Ocean to central Europe (leaving Valentia Observatory at its margin) and positive anomalies in the middle subtropical Atlantic. According to their maps, the negative pole remains geographically fixed throughout the year only varying in intensity, whereas the positive pole varies both in strength and position, being less intense and displaced towards the centre of the subtropical Atlantic in summer. On the other hand, the SCA_{cpc} is essentially a primary positive centre located over Northern Scandinavia at ~70° N (for reference, Bergen Florida station is at 60° N) with weaker negative centres over Western Europe and Russia. In this case, both poles present an almost spatial stationary behaviour with their highest intensity occurring in winter. Thus, the low correlations obtained for the CPC indices and the station-based data (Table 7) could be attributed to the distance between the meteorological stations and their centres of action.

The discrepancies observed between our composite-EOFs and those from the CPC may also be attributed to: (i) the different and shorter time period considered by CPC when performing the RPCA; (ii) the fact that the CPC considers data from all 12 calendar months whereas the EA/SCA patterns are more distinctly developed in wintertime; (iii) the region over which CPC computed the RPCA covers all longitudes from 20 - 90 °N, whereas we have limited our computations to the N. Atlantic region (100°W-40°E, 10°-80°N); (iv) the non-orthogonality of the RPCA; and (v) differences related to the use of SLP or 500-mb heights and/or the accuracy of the reanalysis datasets used.

3.4 Climate impact of the composite EA and SCA series

Figure 8 illustrates the monthly correlation distribution maps between our composite-series (EA_{comp} and SCA_{comp}) versus surface air temperature and precipitation amount for the four seasons (DJF, MAM, JJA and SON) between 1901 and 2016 using the CRU-TS.4.01 dataset (Harris et al. 2014). The strongest correlations are found in winter, when these patterns are more prominent, and are consistent with previous studies (Moore et al, 2011; Comas-Bru and McDermott, 2014; Lim, 2015).

The only European regions for which the EA impacts on precipitation are strong and robust (i.e. on the same direction) throughout the year are the UK and Ireland. The predominantly weak correlations observed in other regions, far from the main centres of action, could arise from the low percentages of variability explained by each EOF pattern (<20% for EA; Table S2). Nevertheless, consistent patterns are observed in terms of precipitation amount across all seasons except in EA_{comp}/JJA, which also shows an anomalous relationship with temperature. We interpret this to be caused by the northerly shift of the EA centre of action in JJA (i.e. between Scotland and Iceland instead of off-shore Ireland; see Table 3 and Figures S3 and S4), that hampers its influence on the western Mediterranean region, which in turn becomes wetter with positive EA modes. Regarding the impact of the SCA on precipitation, a similar pattern with negative correlations in northern Europe and predominantly positive correlations in the circum-Mediterranean region, is observed across seasons, albeit with different strengths. We observe a strong seasonality on the impact of both climate modes on surface air temperature. Weak correlations are found for the all seasons except JJA for the EA with non-significant correlations across all Europe in SON. The opposite is observed for SCA, where the strongest impact on air temperature is shown in DJF (predominantly negative) and SON (predominantly positive).

Due to the low variance explained by both climate modes, they are not expected to imprint a very strong signal on the climate and thus the extent to which these correlations would be reflected in the absolute precipitation and temperature values will primarily depend on the concomitant state of the NAO, the main driver of climate variability in the region (Hurrell and van Loon, 1997; Hurrell and Deser, 2010). In addition, the impact of these atmospheric modes on the climate is not robust throughout the year. For example, none of the datasets used in this study showed a SCA pattern within the three leading EOFs in spring.

Individual EOFs such as the EA and the SCA are statistical constructs that do not necessarily represent a physically independent phenomenon linked (i.e. correlated) to climate variables in a robust manner. Full characterisation of the regional atmospheric dynamics therefore requires multiple EOFs to be taken into account (Roundy, 2015). To thoroughly characterise the climate in the region, the impacts of the EA/SCA should be investigated in conjunction with the NAO (Moore et al., 2011; Comas-Bru and McDermott, 2014; Hall and Hanna, 2018) but this is outside the scope of this study. As far as we are aware, such investigation does not exist outside the winter months.

4 Conclusions

This study presents a new set of indices for the second and third modes of climate variability in the North Atlantic sector (EA_{comp} and SCA_{comp}). These indices have been constructed after identifying the main patterns of variability across five different reanalysis products and have been then compared to the two meteorological stations identified as instrumental series for the EA and the SCA pattern: Valentia Observatory (Ireland) and Bergen Florida (Norway). The high resemblance between our EOF-based indices and these instrumental SLP records during winter allows both indices to be readily updated as required. Beyond this season, however, a more complex picture arises. For example, the Scandinavian pattern is not included within the first three modes of

climate variability during spring and instead, the Western Atlantic pattern as described by Wallace and Gutzler (1981) dominates SLP variability after the NAO, leaving the EA as the third pattern for this season.

Our results also suggest that the difference in methodology/reanalysis products between our composite EOF-based indices and those provided by NOAA-CPC (CPC, 2012) is not relevant for the NAO but it becomes critical for the 2nd and 3rd EOF. However, despite the differences, both sets of indices display very similar and recognisable spatio-temporal patterns at inter-annual timescales (Figs. 3 and 4).

Data availability

The datasets consisting of the instrumental data and the monthly composite indices of NAO, EA and SCA are provided as supplementary material and are also available at https://doi.pangaea.de/10.1594/PANGAEA.892769.

Author contribution:

AH identified the meteorological stations used. LCB developed the scripts and performed the data analysesEOFs. LCB and AHH designed the calculations and carried them out. The manuscript was collaboratively written by both co-authors.

Competing interests:

The authors declare no competing interests.

List of Figures

Figure 1: EOF loadings based on monthly SLP data (20CRv2c dataset; Compo et al., 2011). Each column represents a 3-month season. The percentages at the bottom right of each map are the variability explained by the corresponding EOF (rows) at any given season (columns) as shown in Table S2. The text at the bottom of each map identifies the observed pattern. Pink (purple) dots show the location of Bergen Florida (Valentia Observatory) stations as listed in Table 1. Figures S1-S4 show the same maps for the other four reanalysis products in Table 2.

Figure 2: WinterMonthly (DJF) EOF time-series and their equivalent instrumental records. a) EOF2 and normalised SLP data from Valentia Observatory (Val_{SLP}); b) same than (a) with the EOF3 and SLP data from Bergen Florida (Ber_{SLP}). Correlation coefficients between these time-series are given in Table 4.

Figure 3: <u>Monthly</u> ~~Time~~-series of EA$_{comp}$, the instrumental data (Val$_{SLP}$) and the EA from the CPC (EA$_{CPC}$; CPC, 2012) for each 3-months season. Note that the CPC series has been inversed for an easy visual comparison.

Figure 4: Same as in Fig. 3 for SCA$_{comp}$, instrumental data (Ber$_{SLP}$) and the EA from the CPC (EA$_{CPC}$; CPC, 2012).

Figure 5: Running correlations between our composite series and the instrumental records. (a) EA$_{comp}$ and Val$_{SLP}$; (b) SCA$_{comp}$ and Ber$_{SLP}$. The window size is 30 years <u>and is defined from i to $i+30$, where i is the oldest month</u>. Dashed lines indicate the 0.01 significance thresholds. Note that spring in panel (b) corresponds to the WA index instead of the SCA.

Figure 6: Seasonally averaged EA$_{comp}$ (dashed blue line) and SCA$_{comp}$ (dashed red line) and decadal EA$_{comp}$ (blue solid line) and SCA$_{comp}$ (red solid line). (a) winter (DJF); (b) spring (MAM); (c) summer (JJA); (d) autumn (SON). A 10-year bandpass filter has been used to obtain the decadal series. Note that in (b) the red lines correspond to WA$_{comp}$ instead of SCA$_{comp}$. Note the different y-scale for summer indices. <u>Grey band indicates the period of low confidence of our composite series (see methods section for details).</u>

Figure 7: Running correlations as in Fig. 5 between our composite series and the CPC indices. (a) EA$_{comp}$ and EA$_{CPC}$; (b) SCA$_{comp}$ and SCA$_{CPC}$. The window size is 30 years <u>and is defined from i to $i+30$, where i is the oldest month</u>. Dashed lines indicate the 0.01 significance thresholds.

<u>Figure 8: Correlation distribution maps between the monthly precipitation (top) and surface air temperature (bottom) and our monthly composites (EA$_{comp}$ and SCA$_{comp}$) between 1902 and 2016. Climate data from the CRU-TS4.01 global climate data set (Harris et al. 2014). Positive correlations are shown in red and negative correlations are shown in blue (see colour bar). Correlation coefficients are Spearman Rank coefficients. SCA/MAM maps (marked with an asterisk) correspond to the WA pattern.</u>

List of Tables

Table 1~~.~~<u>:</u> <u>List of the meteorological stations used to construct the monthly instrumental indices. Daily data downloaded from the European Climate Assessment and Dataset (ECA&D; Klein Tank et al., 2002) available at www.ecad.edu (Date of last access: 6<u>th</u> February 2018). In April 2012 the manual station at Valentia was replaced by an automatic station at the same site (Met Éireann, personal communication).</u>
~~List of the meteorological stations used in this study.~~

Table 2: Details of the reanalysis products used in this study.

Table 3: Summary of the geographical structures of the EOF loadings across datasets (columns) and seasons (rows). Superindices indicate which EOFs are included in the composite series: (1) NAO$_{comp}$; (2) EA$_{comp}$; (3) SCA$_{comp}$; (4) WA$_{comp}$. Notes: (i) The NAO in DJF and MAM, presents a southern pole extending towards Europe. In JJA, the southern pole is weak and predominantly shifted northwards. The same pattern is found in SON, except for 20CRv2c and ERA-20C; (ii) "EA with secondary pole" means that a negative pole over Scandinavia is evident; (iii) "Extended SCA" refers to the classic SCA with the positive pole extending towards IRL and UK; and (iv) the Western Atlantic (WA) pattern in MAM/EOF2 is a dipole with a main centre over the N. Atlantic Ocean and a second weak centre over Scandinavia (both negative). See Figures 1 and S1-S4 for the corresponding maps.

Table 4: Correlation coefficients between the ~~first~~ three monthly EOFs for winter (DJF), spring (MAM), summer (JJA) and autumn (SON) and <u>the corresponding monthly</u> Val$_{SLP}$ and Ber$_{SLP}$. Note: all correlations with p-val≤0.01 except (a) 0.01<p-val≤0.05; (b) 0.05<p-val≤0.1; and (c) p-val>0.1.

Table 5: Monthly correlations of our composite indices (EA_{comp} and SCA_{comp}) and the instrumental records (Val_{SLP} and Ber_{SLP}). (*) Spring (MAM) pattern is that of WA. See text for details. Note: all correlations with p-val≤0.01 except (a) 0.01<p-val≤0.05; (b) 0.05<p-val≤0.1; and (c) p-val>0.1.

Table 6: Monthly correlations between the CPC indices (NAOCPC, EACPC and SCACPC) and our composites (NAO_{comp}, EA_{comp} and SCA_{comp}. Note: all correlations with p-val≤0.01 except (a) 0.01<p-val≤0.05; (b) 0.05<p-valv0.1; and (c) p-val>0.1. The SCA only has been compared to the composites for DJF, JJA and SON because spring is showing the WA pattern (see Table 4 and Figs. 1 and S1-S4 for further details).

Table 7: Monthly correlations between the EA_{cpc} and SCA_{cpc} and our station-based indices (Val_{SLP} and Ber_{SLP}). Note: all correlations with p-val≤0.01 except (a) 0.01<p-val≤0.05; (b) 0.05<p-val≤0.1; and (c) p-val>0.

References

Aguilar, E., Auer, I., Brunet, M., Peterson, T., and Wieringa, J.: Guidelines on climate metadata and homogenization. World Climate Programme Data and Monitoring WCDMP-No. 53, WMO-TD No. 1186, World Meteorological Organization, Geneva, 55, 2003.

Barnston, A. G. and Livezey, R. E.: Classification, Seasonality and Persistence of Low-Frequency Atmospheric Circulation Patterns, Monthly Weather Review, 115, 1083-1126, 1987. https://doi.org/10.1175/1520-0493(1987)115<1083:CSAPOL>2.0.CO;2

Bastos, A., Janssens, I. A., Gouveia, C. M., Trigo, R. M., Ciais, P., Chevallier, F., Peñuelas, J., Rödenbeck, C., Piao, S., Friedlingstein, P., and Running, S. W.: European land CO2 sink influenced by NAO and East-Atlantic Pattern coupling, Nature Communications, 7, 10315, 2016. https://doi.org/10.1038/ncomms10315

Blade, I., Liebmann, B., Fortuny, D., and van Oldenborgh, G. J.: Observed and simulated impacts of the summer NAO in Europe: implications for projected drying in the Mediterranean region, Climate Dynamics, 39, 709-727, 2012. https://doi.org/10.1007/s00382-011-1195-x

Bueh, C. and Nakamura, H.: Scandinavian pattern and its climatic impact, Quarterly Journal of the Royal Meteorological Society, 133, 2117-2131, 2007. https://doi.org/10.1002/qj.173

Comas-Bru, L. and McDermott, F.: Impacts of the EA and SCA patterns on the European twentieth century NAO-winter climate relationship, Quarterly Journal of the Royal Meteorological Society, 140, 354-363, 2014. https://doi.org/10.1002/qj.2158

Comas-Bru, L., McDermott, F., and Werner, M.: The effect of the East Atlantic pattern on the precipitation delta O-18-NAO relationship in Europe, Climate Dynamics, 47, 2059-2069, 2016. https://doi.org/10.1007/s00382-015-2950-1

Compo, G. P., Whitaker, J. S., Sardeshmukh, P. D., Matsui, N. , Allan, R. J., Yin, X. , Gleason, B. E., Vose, R. S., Rutledge, G. , Bessemoulin, P. , Brönnimann, S. , Brunet, M. , Crouthamel, R. I., Grant, A. N., Groisman, P. Y., Jones, P. D., Kruk, M. C., Kruger, A. C., Marshall, G. J., Maugeri, M. , Mok, H. Y., Nordli, Ø. , Ross, T. F., Trigo, R. M., Wang, X. L., Woodruff, S. D. and Worley, S. J.Compo, G. P., S., W. J., D., S. P., N., M., J., A. R., X., Y., E., G. B., S., V. R., G., R., P., B., S., B., M., B., I., C. R., N., G. A., Y., G. P., D., J. P., C., K. M., C., K. A., J., M. G., M., M., Y., M. H., Ø., N., F., R. T., M., T. R., L., W. X., D., W. S., and J., W. S.: The Twentieth Century Reanalysis Project, Quarterly Journal of the Royal Meteorological Society, 137, 1-28, 2011. https://doi.org/10.1002/qj.776

CPC, 2012. Northern Hemisphere Teleconnection Patterns. Climate Prediction Centre, US National Oceanic and Atmospheric Administration. http://www.cpc.ncep.noaa.gov/data/teledoc/telecontents.shtml (last access: 26 February 2018)~~CPC: http://www.cpc.ncep.noaa.gov/data/teledoc/telecontents.shtml, 2012.~~

Cradden, L. C. and McDermott, F.: A weather regime characterisation of Irish wind generation and electricity demand in winters 2009-11, Environmental Research Letters, 13, 2018. https://doi.org/10.1088/1748-9326/aabd40

Crasemann, B., Handorf, D., Jaiser, R., Dethloff, K., Nakamura, T., Ukita, J., and Yamazaki, K.: Can preferred atmospheric circulation patterns over the North-Atlantic-Eurasian region be associated with arctic sea ice loss?, Polar Science, 14, 9-20, 2017. https://doi.org/10.1016/j.polar.2017.09.002

Cropper, T., Hanna, E., Valente, M. A., and Jónsson, T.: A daily Azores–Iceland North Atlantic Oscillation index back to 1850, Geoscience Data Journal, 2, 12-24, 2015. https://doi.org/10.1002/gdj3.23

Dee, D. P., Uppala, S. M., Simmons, A. J., Berrisford, P. , Poli, P. , Kobayashi, S. , Andrae, U. , Balmaseda, M. A., Balsamo, G. , Bauer, P. , Bechtold, P. , Beljaars, A. C., van de Berg, L. , Bidlot, J. , Bormann, N. , Delsol, C. , Dragani, R. , Fuentes, M. , Geer, A. J., Haimberger, L. , Healy, S. B., Hersbach, H. , Hólm, E. V., Isaksen, L. , Kållberg, P. , Köhler, M. , Matricardi, M. , McNally, A. P., Monge-Sanz, B. M., Morcrette, J. , Park, B. , Peubey, C. , de Rosnay, P. , Tavolato, C. , Thépaut, J. and Vitart, F~~Dee, D. P., M., U. S., J., S. A., P., B., P., P., S., K., U., A., A., B. M., G., B., P., B., P., B., M., B. A. C., L., v. d. B., J., B., N., B., C., D., R., D., M., F., J., G. A., L., H., B., H. S., H., H., V., H. E., L., I., P., K., M., K., M., M., P., M. A., M., M. S. B., J. J., M., B. K., P., C., P., P., d. R., C., T., J. N., T., and F., V.~~: The ERA-Interim reanalysis: configuration and performance of the data assimilation system, Quarterly Journal of the Royal Meteorological Society, 137, 553-597, 2011. https://doi.org/10.1002/qj.828

Dommenget, D., Latif, M.: A cautionary note on the interpretation of EOFs. Journal of Climate, 15, 216–225, 2002. https://doi.org/10.1175/1520-0442(2002)015<0216:ACNOTI>2.0.CO;2

Ebisuzaki, W.: A method to estimate the statistical significance of a correlation when the data are serially correlated, Journal of Climate, 10, 2147-2153, 1997. https://doi.org/10.1175/1520-0442(1997)010<2147:AMTETS>2.0.CO;2

Folland, C. K., Knight, J., Linderholm, H. W., Fereday, D., Ineson, S., and Hurrell, J. W.: The Summer North Atlantic Oscillation: Past, Present, and Future, Journal of Climate, 22, 1082-1103, 2009. https://doi.org/10.1175/2008JCLI2459.1

Fujiwara, M., Wright, J. S., Manney, G. L., Gray, L. J., Anstey, J., Birner, T., Davis, S., Gerber, E. P., Harvey, V. L., Hegglin, M. I., Homeyer, C. R., Knox, J. A., Krüger, K., Lambert, A., Long, C. S., Martineau, P., Molod, A., Monge-Sanz, B. M., Santee, M. L., Tegtmeier, S., Chabrillat, S., Tan, D. G. H., Jackson, D. R., Polavarapu, S., Compo, G. P., Dragani, R., Ebisuzaki, W., Harada, Y., Kobayashi, C., McCarty, W., Onogi, K., Pawson, S., Simmons, A., Wargan, K., Whitaker, J. S., and Zou, C.-Z.: Introduction to the SPARC Reanalysis Intercomparison Project (S-RIP) and overview of the reanalysis systems, Atmos. Chem. Phys., 17, 1417-1452, 2017. https://doi.org/10.5194/acp-17-1417-2017

Hall, R.J., Hanna, E.: North Atlantic circulation indices: links with summer and winter UK temperatures and precipitation and implications for seasonal forecasting. International Journal of Climatology 38 (Suppl.1): e660 – e677, 2018. https://doi.org/10.1002/joc.5398

Harris, I., Jones, P.D., Osborn, T.J. and Lister, D.H.: Updated high-resolution grids of monthly climatic observations – the CRU TS3.10 Dataset. International Journal of Climatology, 34: 623–642, 2014. doi: 10.1002/joc.3711

Hernández, A., Kutiel, H., Trigo, R. M., Valente, M. A., Sigró, J., Cropper, T., and Espírito-Santo, F.: New Azores archipelago daily precipitation dataset and its links with large-scale modes of climate variability, International Journal of Climatology, 36, 4439-4454, 2016. https://doi.org/10.1002/joc.4642

Hurrell, J. W.: Decadal trends in the north atlantic oscillation: regional temperatures and precipitation, Science, 269, 676-679, 1995. https://doi.org/10.1126/science.269.5224.676.

Hurrell, J. W. and Deser, C.: North Atlantic climate variability: The role of the North Atlantic Oscillation, Journal of Marine Systems, 79, 231-244, 2010. https://doi.org/10.1016/j.jmarsys.2008.11.026

Hurrell, J. W., Kushnir, Y. , Ottersen, G. and Visbeck, M. An Overview of the North Atlantic Oscillation. In The North Atlantic Oscillation: Climatic Significance and Environmental Impact (eds J. W. Hurrell, Y. Kushnir, G. Ottersen and M. Visbeck). 2013. https://doi.org/10.1029/134GM01Hurrell, J. W., Kushnir, Y., Ottersen, G., and Visbeck, M.: An Overview of the North Atlantic Oscillation, 2003.

Hurrell, J. W. and VanLoon, H.: Decadal variations in climate associated with the north Atlantic oscillation, Climatic Change, 36, 301-326, 1997. https://doi.org/10.1023/A:1005314315270

Jerez, S. and Trigo, R. M.: Time-scale and extent at which large-scale circulation modes determine the wind and solar potential in the Iberian Peninsula, Environmental Research Letters, 8, 2013. https://doi.org/10.1088/1748-9326/8/4/044035

Jones PD, Jónsson T, Wheeler D.: Extension to the North Atlantic Oscillation using early instrumental pressure observations from Gibraltar and south-west Iceland. International. Journal. of Climatology. 17: 1433 – 1450, 1997. https://doi.org/10.1002/(SICI)1097-0088(19971115)17:13<1433::AID-JOC203>3.0.CO;2-P

Josey, S. A. and Marsh, R.: Surface freshwater flux variability and recent freshening of the North Atlantic in the eastern subpolar gyre, Journal of Geophysical Research: Oceans, 110, 2005. https://doi.org/10.1029/2004JC002521

Kalnay, E., Kanamitsu, M., Kistler, R., Collins, W., Deaven, D., Gandin, L., Iredell, M., Saha, S., White, G., Woollen, J., Zhu, Y., Chelliah, M., Ebisuzaki, W., Higgins, W., Janowiak, J., Mo, K. C., Ropelewski, C., Wang, J., Leetmaa, A., Reynolds, R., Jenne, R., and Joseph, D.: The NCEP/NCAR 40-Year Reanalysis Project, Bulletin of the American Meteorological Society, 77, 437-472, 1996. https://doi.org/10.1175/1520-0477(1996)077<0437:TNYRP>2.0.CO;2

Klein Tank, A. M., Wijngaard, J. B., Können, G. P., Böhm, R. , Demarée, G. , Gocheva, A. , Mileta, M. , Pashiardis, S. , Hejkrlik, L. , Kern-Hansen, C. , Heino, R. , Bessemoulin, P. , Müller-Westermeier, G. , Tzanakou, M. , Szalai, S. , Pálsdóttir, T. , Fitzgerald, D. , Rubin, S. , Capaldo, M. , Maugeri, M. , Leitass, A. , Bukantis, A. , Aberfeld, R. , van Engelen, A. F., Forland, E. , Mietus, M. , Coelho, F. , Mares, C. , Razuvaev, V. , Nieplova, E. , Cegnar, T. , Antonio López, J. , Dahlström, B. , Moberg, A. , Kirchhofer, W. , Ceylan, A. , Pachaliuk, O. , Alexander, L. V. and Petrovic, PKlein Tank, A. M. G., B., W. J., P., K. G., R., B., G., D., A., G., M., M., S., P., L., H., C., K. H., R., H., P., B., G., M. W., M., T., S., S., T., P., D., F., S., R., M., C., M., M., A., L., A., B., R., A., V., v. E. A. F., E., F., M., M., F., C., C., M., V., R., E., N., T., C., J., A. L., B., D., A., M., W., K., A., C., O., P., V., A. L., and P., P.: Daily dataset of 20th-century surface air temperature and precipitation series for the

European Climate Assessment, International Journal of Climatology, 22, 1441-1453, 2002. https://doi.org/10.1002/joc.773

Lehner, F., Raible, C. C., and Stocker, T. F.: Testing the robustness of a precipitation proxy-based North Atlantic Oscillation reconstruction, Quaternary Science Reviews, 45, 85-94, 2012. https://doi.org/10.1016/j.quascirev.2012.04.025

Lim, Y.-K.: The East Atlantic/West Russia (EA/WR) teleconnection in the North Atlantic: climate impact and relation to Rossby wave propagation, Climate Dynamics, 44(11), 3211-3222. https://doi.org/10.1007/s00382-014-2381-4

Moore, G. W. K., Pickart, R. S., and Renfrew, I. A.: Complexities in the climate of the subpolar North Atlantic: a case study from the winter of 2007, Quarterly Journal of the Royal Meteorological Society, 137, 757-767, 2011. https://doi.org/10.1002/qj.778

Moore, G. W. K. and Renfrew, I. A.: Cold European winters: interplay between the NAO and the East Atlantic mode, Atmospheric Science Letters, 13, 1-8, 2012. https://doi.org/10.1002/asl.356

Moore, G. W. K., Renfrew, I. A., and Pickart, R. S.: Multidecadal Mobility of the North Atlantic Oscillation, Journal of Climate, 26, 2453-2466, 2013. https://doi.org/10.1175/JCLI-D-12-00023.1

North, G. R., Bell, T. L., Cahalan, R. F., and Moeng, F. J.: Sampling Errors in the Estimation of Empirical Orthogonal Functions, Monthly Weather Review, 110, 699-706, 1982. https://doi.org/10.1175/1520-0493(1982)110<0699:SEITEO>2.0.CO;2

Pielke, R. J., Prins, G., Rayner, S., and Sarewitz, D.: Lifting the taboo on adaptation, Nature, 445, 597, 2007. https://doi.org/10.1038/445597a

Pinto, J. G. and Raible, C. C.: Past and recent changes in the North Atlantic oscillation, Wiley Interdisciplinary Reviews: Climate Change, 3, 79-90, 2012. https://doi.org/10.1002/wcc.150

Poli, P., Hersbach, H., Dee, D. P., Berrisford, P., Simmons, A. J., Vitart, F., Laloyaux, P., Tan, D. G. H., Peubey, C., Thépaut, J.-N., Trémolet, Y., Hólm, E. V., Bonavita, M., Isaksen, L., and Fisher, M.: ERA-20C: An Atmospheric Reanalysis of the Twentieth Century, Journal of Climate, 29, 4083-4097, 2016. https://doi.org/10.1175/JCLI-D-15-0556.1

Rodríguez-Puebla, C. and Nieto, S.: Trends of precipitation over the Iberian Peninsula and the North Atlantic Oscillation under climate change conditions, International Journal of Climatology, 30, 1807-1815, 2010. https://doi.org/10.1002/joc.2035

Rogers, J. C.: The Association between the North Atlantic Oscillation and the Southern Oscillation in the Northern Hemisphere, Monthly Weather Review, 112, 1999-2015, 1984. https://doi.org/10.1175/1520-0493(1984)112<1999:TABTNA>2.0.CO;2

Roundy, P.E.: On the interpretation of EOF analysis of ENSO, atmospheric Kelvin waves, and the MJO. Journal of Climate, 28, 1148–1165, 2015.

Scherrer, S. C., Appenzeller, C., Liniger, M. A., and Schär, C.: European temperature distribution changes in observations and climate change scenarios, Geophysical Research Letters, 32, 2005. https://doi.org/10.1029/2005GL024108

Trenberth, K. E. and Jones, P. D.: Observations: Surface and Atmospheric Climate Change, Cambridge Univ Press, New York, 2007.

Trewin, B.: Exposure, instrumentation, and observing practice effects on land temperature measurements, Wiley Interdisciplinary Reviews: Climate Change, 1, 490-506, 2010. https://doi.org/10.1002/wcc.46

Uppala, S. M., Kallberg, P. W., Simmons, A. J., Andrae, U., Bechtold, V. D., Fiorino, M., Gibson, J. K., Haseler, J., Hernandez, A., Kelly, G. A., Li, X., Onogi, K., Saarinen, S., Sokka, N., Allan, R. P., Andersson, E., Arpe, K., Balmaseda, M. A., Beljaars, A. C. M., Van De Berg, L., Bidlot, J., Bormann, N., Caires, S., Chevallier, F., Dethof, A., Dragosavac, M., Fisher, M., Fuentes, M., Hagemann, S., Holm, E., Hoskins, B. J., Isaksen, L., Janssen, P., Jenne, R., McNally, A. P., Mahfouf, J. F., Morcrette, J. J., Rayner, N. A., Saunders, R. W., Simon, P., Sterl, A., Trenberth, K. E., Untch, A., Vasiljevic, D., Viterbo, P., and Woollen, J.: The ERA-40 re-analysis, Quarterly Journal of the Royal Meteorological Society, 131, 2961-3012, 2005. https://doi.org/10.1256/qj.04.176

Wallace, J. M. and Gutzler, D. S.: Teleconnections in the Geopotential Height Field during the Northern Hemisphere Winter, Monthly Weather Review, 109, 784-812, 1981. https://doi.org/10.1175/1520-0493(1981)109<0784:TITGHF>2.0.CO;2

Wallbrink, H., F. Koek, and T. Brandsma, 2009: The US Maury Collection Metadata 1796-1861. KNMI-225/HISKLIM-11. http://bibliotheek.knmi.nl/knmipubmetnummer/knmipub225.pdf

Wang, Y. H., Magnusdottir, G., Stern, H., Tian, X., and Yu, Y. M.: Uncertainty Estimates of the EOF-Derived North Atlantic Oscillation, Journal of Climate, 27, 1290-1301, 2014.

Wanner, H., Bronnimann, S., Casty, C., Gyalistras, D., Luterbacher, J., Schmutz, C., Stephenson, D. B., and Xoplaki, E.: North Atlantic Oscillation - Concepts and studies, Surveys in Geophysics, 22, 321-382, 2001.

Woodruff, S.D., H.F. Diaz, S.J. Worley, R.W. Reynolds, and S.J. Lubker, 2005: Early ship observational data and ICOADS. Climatic Change, 73, 169-194. https://doi.org/10.1007/s10584-005-3456-3).

Woollings, T., Hannachi, A., Hoskins, B., and Turner, A.: A Regime View of the North Atlantic Oscillation and Its Response to Anthropogenic Forcing, Journal of Climate, 23, 1291-1307, 2010.

Zubiate, L., McDermott, F., Sweeney, C., and O'Malley, M.: Spatial variability in winter NAO-wind speed relationships in western Europe linked to concomitant states of the East Atlantic and Scandinavian patterns, Quarterly Journal of the Royal Meteorological Society, 143, 552-562, 2017.
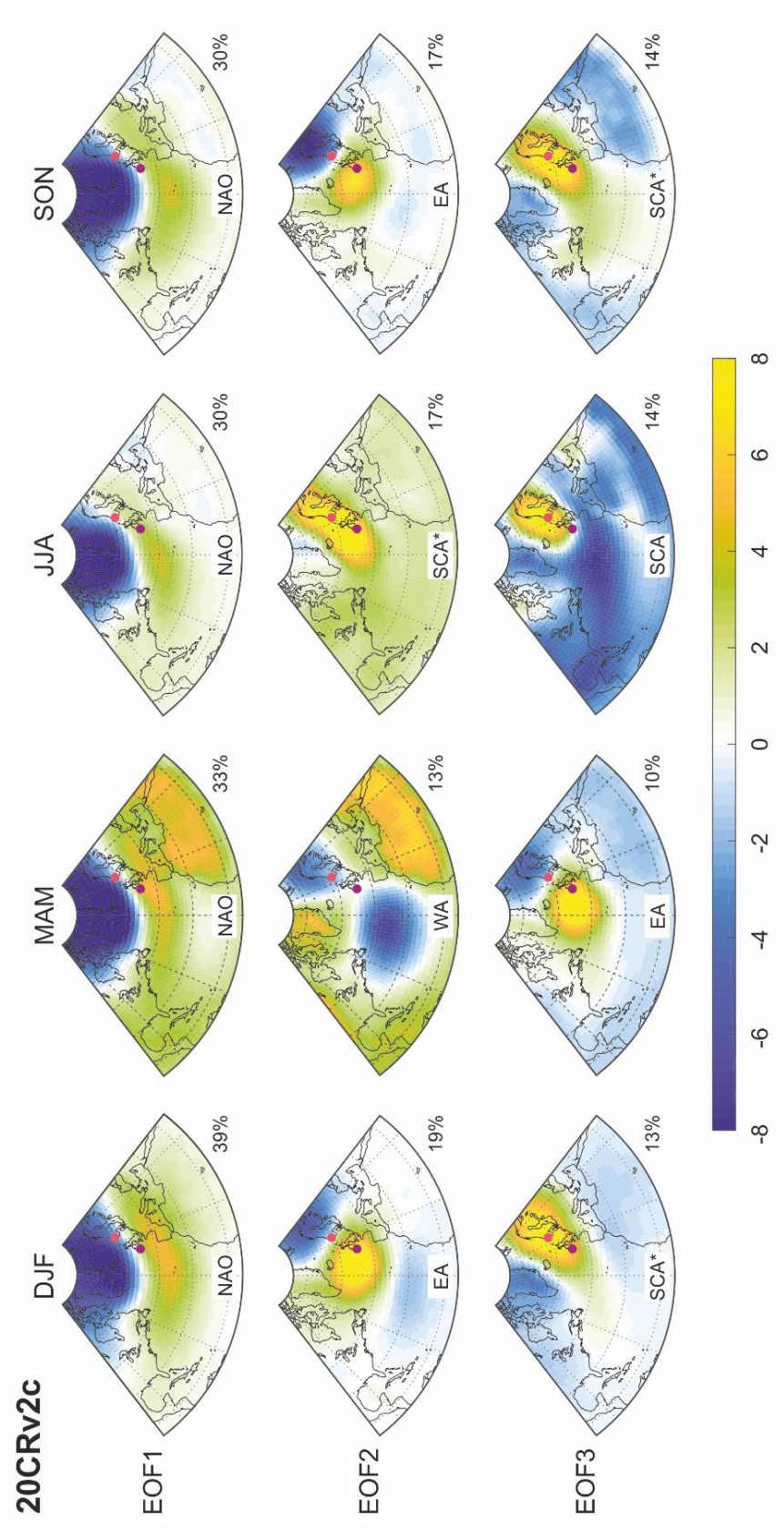
28

Figure 1: EOF loadings based on monthly SLP data (20CRv2c dataset; Compo et al., 2011). Each column represents a 3-month season. The percentages at the bottom right of each map are the variability explained by the corresponding EOF (rows) at any given season (columns) as in Table S2. The text at the bottom of each map identifies the observed pattern. Pink (purple) dots show the location of Bergen Florida (Valentia Observatory) stations as listed in Table 1. Figures S1-S4 show the same maps for the other four reanalysis products in Table 2.
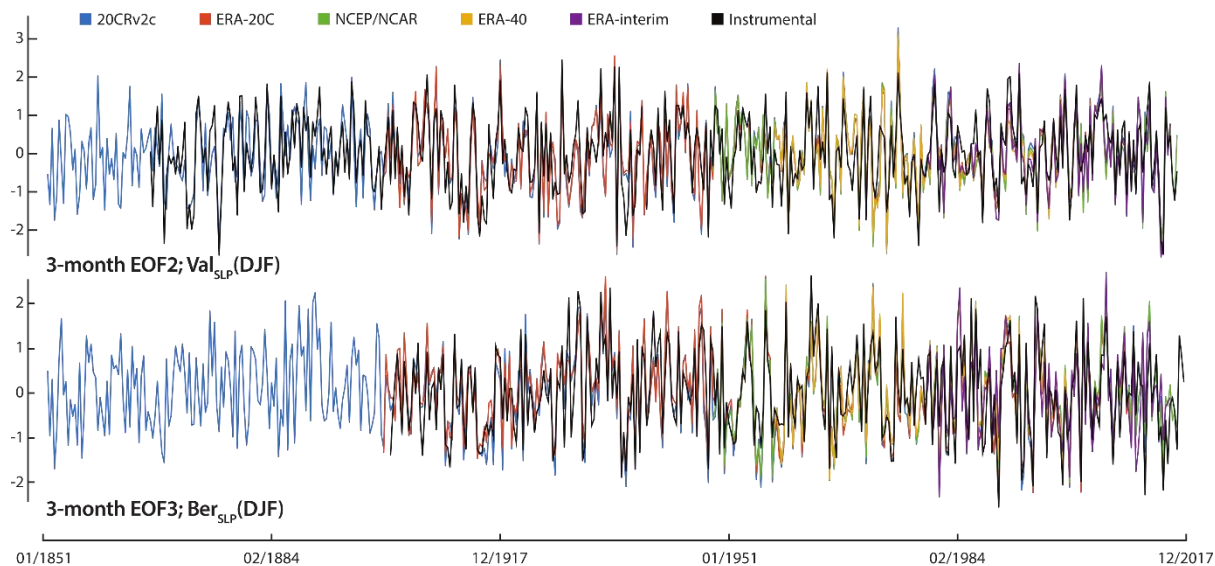
Figure 2: ~~Winter~~ <u>Monthly</u> (DJF) EOF time-series and their equivalent instrumental records. a) EOF2 and <u>normalised</u> SLP data from Valentia Observatory (Val$_{SLP}$); b) same than (a) with the EOF3 and SLP data from Bergen Florida (Ber$_{SLP}$). Correlation coefficients between these time-series are given in Table 4.
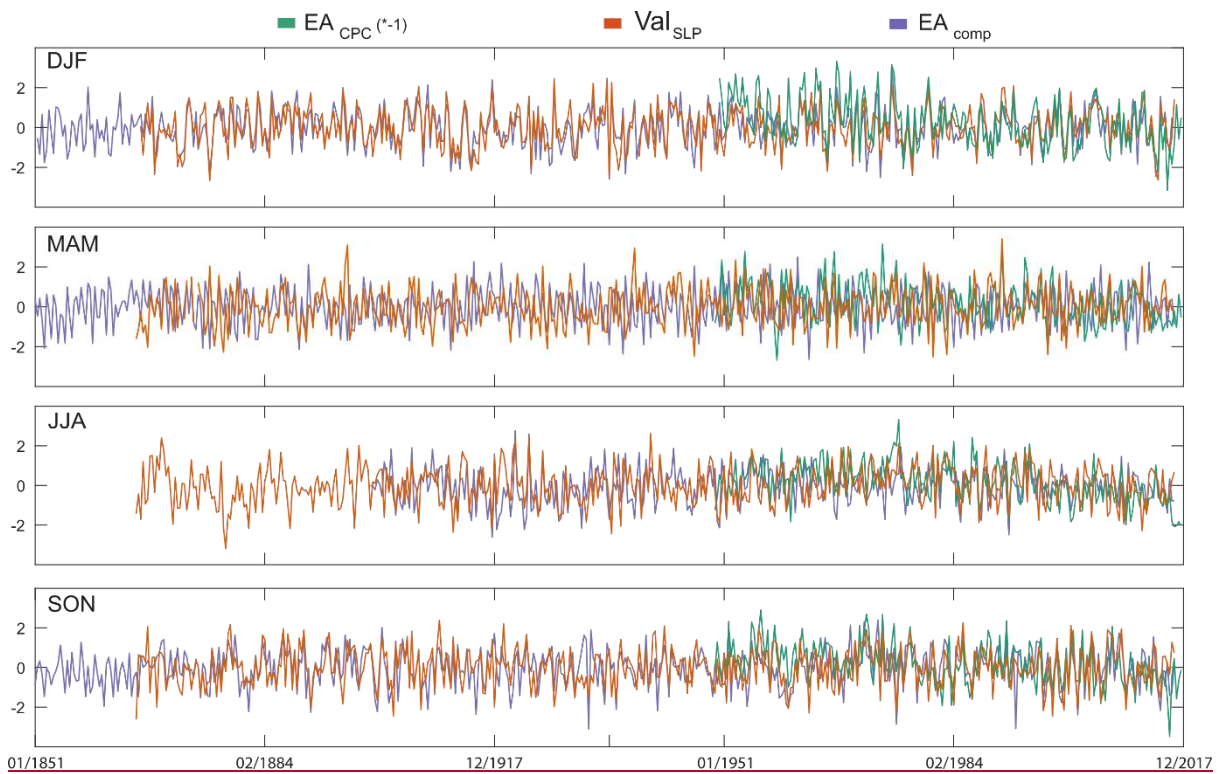
20

Figure 3: **Monthly** ~~Time~~ series of EA_{comp}, the instrumental data (Val_{SLP}) and the EA from the CPC (EA_{CPC}; CPC, 2012) for each 3-months season. Note that the CPC series has been inversed for an easy visual comparison.
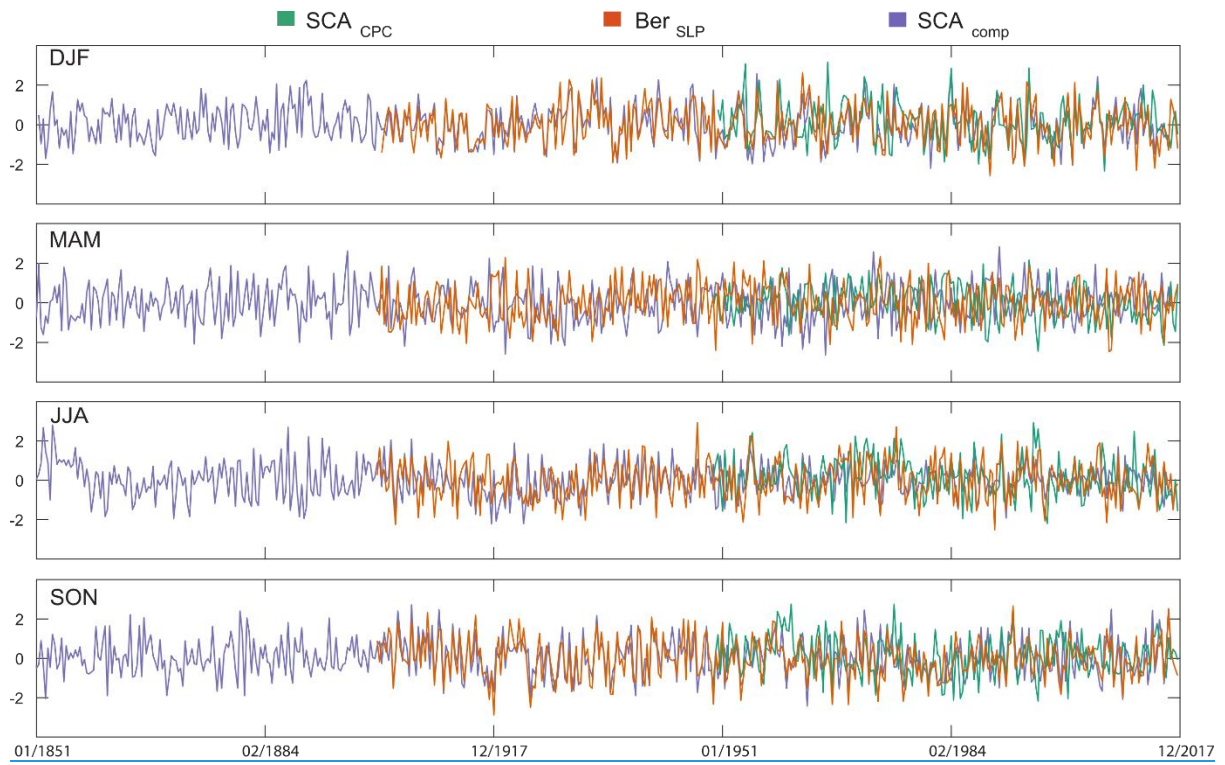
Figure 4: Same as in Fig. 3 for SCA$_{comp}$, instrumental data (Ber$_{SLP}$) and the EA from the CPC (EA$_{CPC}$; CPC, 2012).

91

92

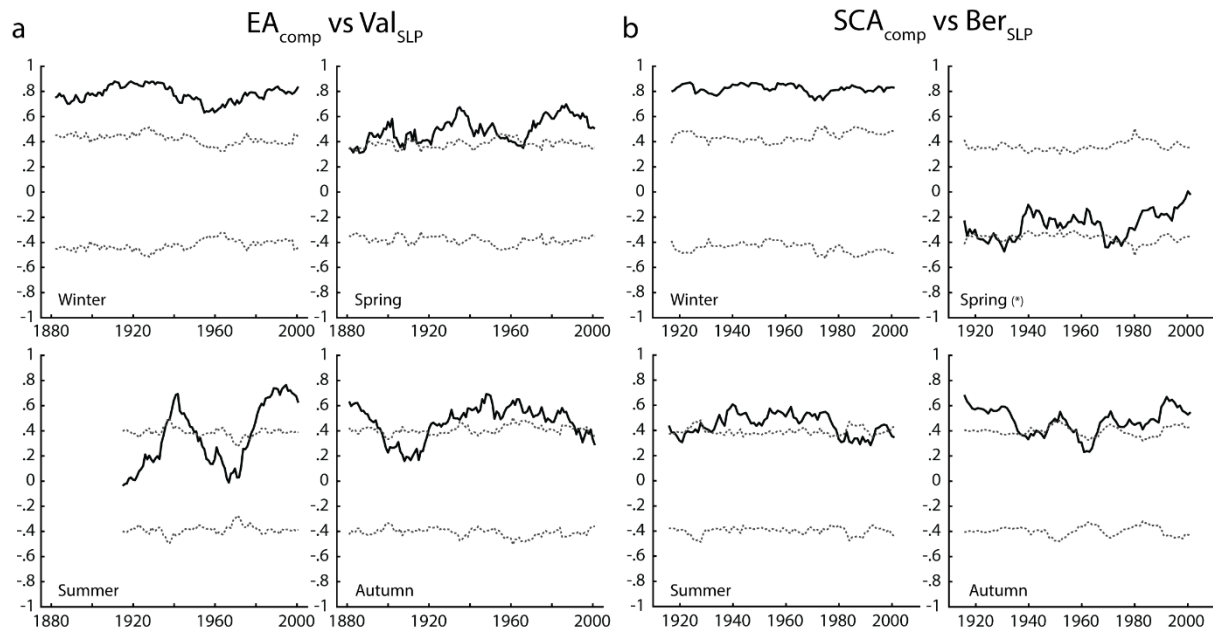93 **Figure 5: Running correlations between our composite series and the instrumental records. (a) EA$_{comp}$ and Val$_{SLP}$; (b)**
94 **SCA$_{comp}$ and Ber$_{SLP}$. The window size is 30 years <u>and is defined from *i* to *i+30*, where *i* is the oldest month</u>. Dashed lines**
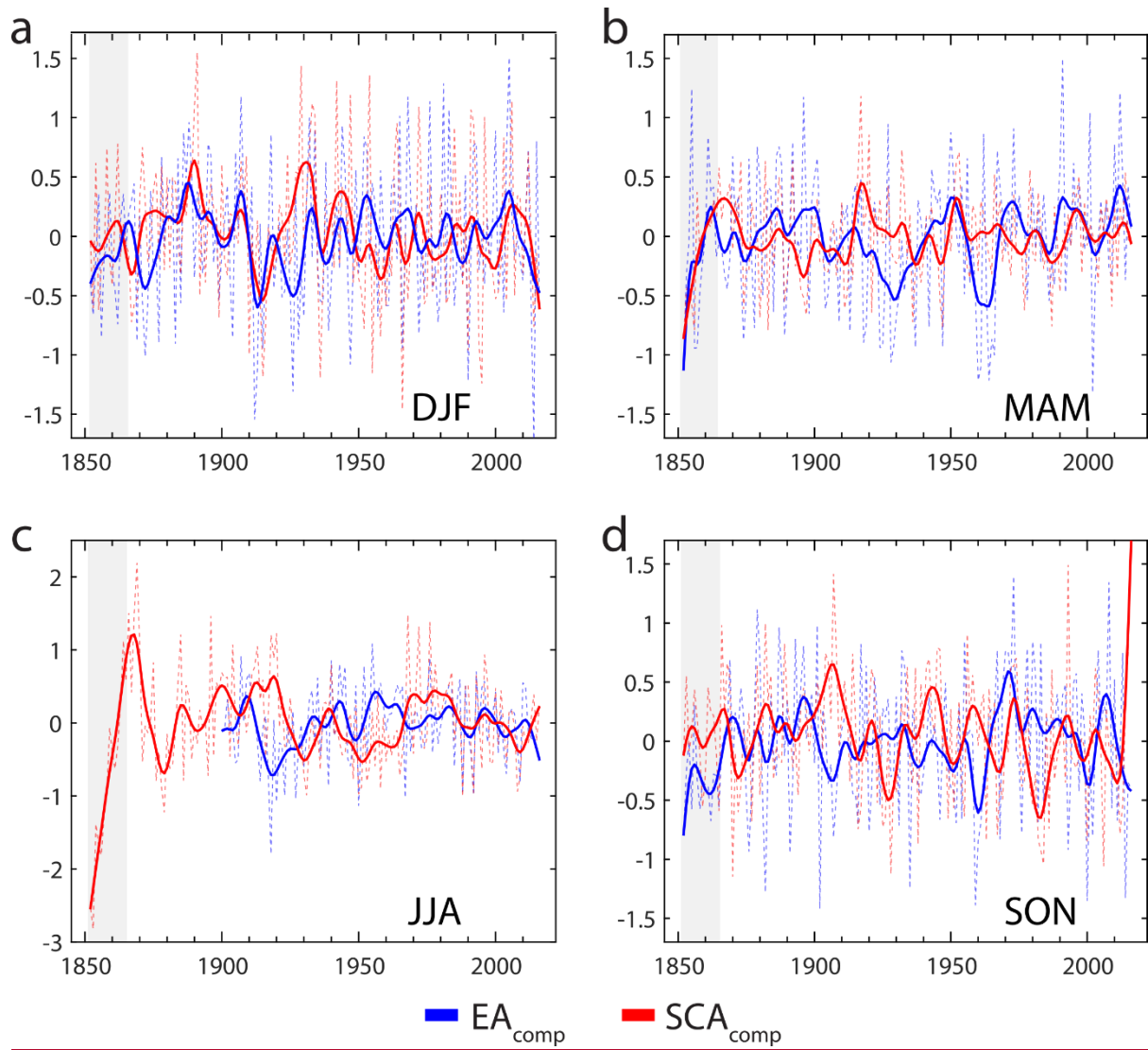95 **indicate the 0.01 significance thresholds. Note that spring in panel (b) corresponds to the WA index instead of the SCA.**

Figure 6: Seasonally averaged EA$_{comp}$ (dashed blue line) and SCA$_{comp}$ (dashed red line) and decadal EA$_{comp}$ (blue solid line) and SCA$_{comp}$ (red solid line). (a) winter (DJF); (b) spring (MAM); (c) summer (JJA); (d) autumn (SON). A 10-year bandpass filter has been used to obtain the decadal series. Note that in (b) the red lines correspond to WA$_{comp}$ instead of SCA$_{comp}$. Note the different y-scale for summer indices. Grey band indicates the period of low confidence of our composite series (see methods section for details).
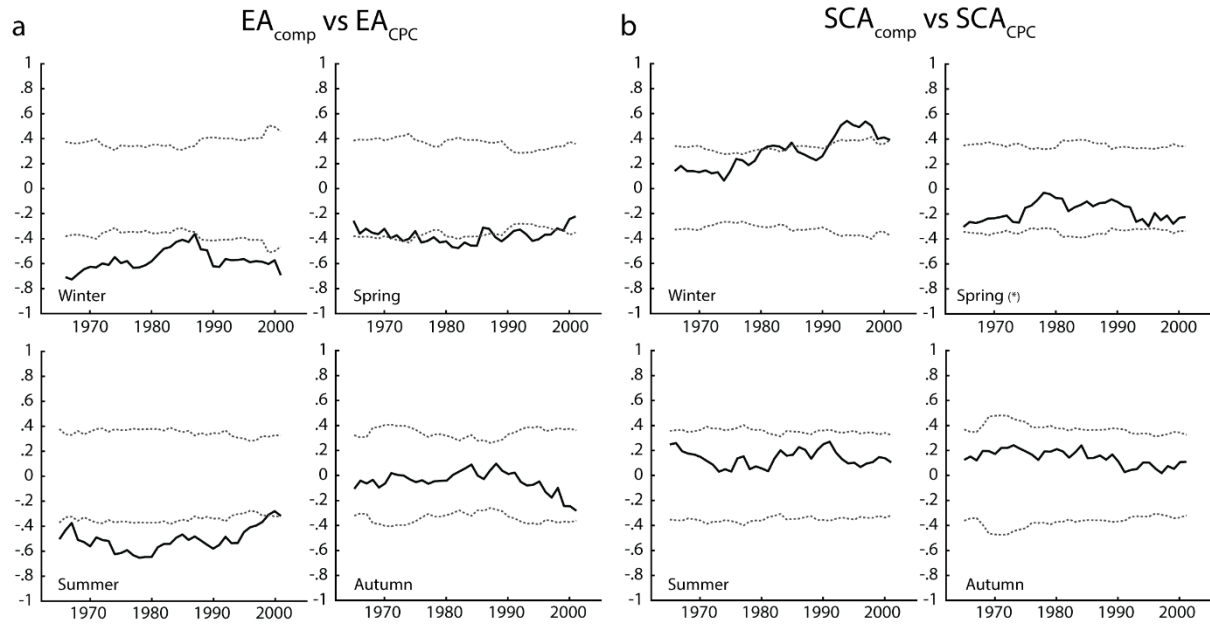
Figure 7: Running correlations as in Fig. 5 between our composite series and the CPC indices. (a) EA$_{comp}$ and EA$_{CPC}$; (b) SCA$_{comp}$ and SCA$_{CPC}$. The window size is 30 years and is defined from *i* to *i+30*, where *i* is the oldest month. Dashed lines indicate the 0.01 significance thresholds.

Figure 8: Correlation distribution maps between the monthly precipitation (top) and surface air temperature (bottom) and our monthly composites (EA_comp and SCA_comp) between 1902 and 2016. Climate data from the CRU-TS4.01 global climate data set (Harris et al. 2014). Positive correlations are shown in red and negative correlations are shown in blue (see colour bar). Correlation coefficients are Spearman Rank coefficients. SCA_comp/MAM maps (marked with an asterisk) correspond to the WA pattern.

Table 1. List of the meteorological stations used to construct the monthly instrumental indices. Daily data downloaded

from the European Climate Assessment and Dataset (ECA&D; Klein Tank et al., 2002) available at www.ecad.edu

(Date of last access: 6th February 2018). In April 2012 the manual station at Valentia was replaced by an automatic

station at the same site (Met Éireann, personal communication).

Station name	WMO Code	Coordinates	Altitude (m)	Time period	# missing data	Original data type	Source
Valentia Observatory	**305/2275**	**51.94°N 10.22°W**	**9**	**01/10/1939- 31/12/2016**	**1**	**Daily**	**European Climate Assessment and Dataset (Klein Tank et al., 2002)**
Valentia Observatory	**3953**	**51.93°N 10.25°W**	**14**	**01/1866- 05/2002**	**4**	**Monthly**	**Met Éireann**
Bergen Florida	**265**	**60.38°N 5.33°E**	**12**	**01/01/1901- 31/12/2017**	**0**	**Daily**	**European Climate Assessment and Dataset (Klein Tank et al., 2002)**

163   Table 1. List of the meteorological stations used in this study.

Station name	WMO Code	Coordinates	Altitude (m)	Time period	# missing data	Original data type	Source
Valentia Observatory	3953	51.93°N 10.23°W	14	01/10/1939 31/12/2016	1	Daily	Met Éireann
Valentia Observatory	3953	51.93°N 10.23°W	14	1866-2013	4	Monthly	Met Éireann
Bergen Florida	50540	60.38°N 5.33° E	12	01/01/1901 31/10/2016	0	Daily	European Climate Assessment and Dataset (Klein Tank et al., 2002)

164

165 **Table 2. Details of the reanalysis products used in this study.**

Dataset	Description	Period		Spatial coverage (lat x lon)	Reference
20CRv2c	NOAA-CIRES Reanalysis dataset based on data-assimilation and surface observations of synoptic pressure	1/1851 12/2014	–	2° x 2°	Compo et al. (2011)
NCEP/NCAR Reanalysis 1	Reanalysis dataset based on an analysis and forecast system to perform data assimilation using past data.	1/1948 31/2016	–	2.5° x 2.5°	Kalnay et al. (1996)
ERA-interim	ECMWF Global Reanalysis Data	1/1979 11/2016	–	0.75° x 0.75°	Dee et al. (2011)
ERA-20C	ECMWF Reanalysis of the 20th-century using surface observations only	1/1900 12/2010	–	1.125° x 1.125°	Poli et al. (2016)
ERA-40	ECMWF Global Reanalysis Data	9/1957 8/2002	–	1.125° x 1.125°	Uppala et al. (2005)

166

Table 3: Summary of the geographical structures of the EOF loadings across datasets (columns) and seasons (rows). Superindices indicate which EOFs are included in the composite series: [1] NAO$_{comp}$; [2] EA$_{comp}$; [3] SCA$_{comp}$; [4] WA$_{comp}$. Notes: (i) The NAO in DJF and MAM, presents a southern pole extending towards Europe. In JJA, the southern pole is weak and predominantly shifted northwards. The same pattern is found in SON, except for 20CRv2c and ERA-20C; (ii) "EA with secondary pole" means that a negative pole over Scandinavia is evident; (iii) "Extended SCA" refers to the classic SCA with the positive pole extending towards IRL and UK; ~~and~~ (iv) the Western Atlantic (WA) pattern in MAM/EOF2 is a dipole with a main centre over the N. Atlantic Ocean and a second weak centre over Scandinavia (both negative); and (v) note that no EA pattern is observed in 20CRv2c during JJA, which results in a shorter EA$_{comp}$ for this season. See Figures 1 and S1-S4 for the corresponding maps.

Season	EOF	20CRv2c	ERA-20C	ERA-40	ERA-interim	NCEP/NCAR
DJF	EOF1	NAO [1]	NAO [1]	NAO [1]	NAO [1]	NAO [1]
DJF	EOF2	EA with secondary pole [2]	EA with secondary pole [2]	EA with secondary pole [2]	EA with secondary pole [2]	EA with secondary pole [2]
DJF	EOF3	Extended SCA [3]	Extended SCA towards N. Europe [3]	Extended SCA towards N. Europe [3]	Extended SCA towards N. Europe [3]	Extended SCA towards N. Europe [3]
MAM	EOF1	NAO [1]	NAO [1]	NAO [1]	NAO [1]	NAO [1]
MAM	EOF2	WA [4]	WA [4]	WA [4]	WA [4]	WA [4]
MAM	EOF3	EA with secondary pole [2]	EA with secondary pole [2]	EA with secondary pole [2]	EA with secondary pole [2]	EA with secondary pole [2]
JJA	EOF1	NAO [1]	NAO [1]	NAO [1]	NAO [1]	NAO [1]
JJA	EOF2	Extended SCA [3]	Extended SCA [3]	Extended SCA [3]	EA (shifted to the North) [2]	Extended SCA [3]
JJA	EOF3	SCA	EA [2]	SCA	Extended SCA [3]	EA (shifted to the North) [2]
SON	EOF1	NAO [1]	NAO [1]	NAO [1]	NAO [1]	NAO [1]
SON	EOF2	EA with secondary pole [2]	EA with secondary pole [2]	EA with secondary pole [2]	EA with secondary pole [2]	EA with secondary pole [2]
SON	EOF3	Extended SCA [3]	Extended SCA [3]	Extended SCA [3]	Extended SCA [3]	Extended SCA towards N. Atlantic ocean [3]

Table 4: Correlation coefficients between the ~~first~~ three monthly EOFs for winter (DJF), spring (MAM), summer (JJA) and autumn (SON) and <u>the corresponding monthly</u> Val$_{SLP}$ and Ber$_{SLP}$. Note: all correlations with p-val≤0.01 except (a) 0.01<p-val≤0.05; (b) 0.05<p-val≤0.1; and (c) p-val>0.1.

		20CRv2			ERA-20C			ERA-40			ERA-interim			NCEP/NCAR		
		EOF1	EOF2	EOF3	EOF1	EOF2	EOF3	EOF1	EOF2	EOF3	EOF1	EOF2	EOF3	EOF1	EOF2	EOF3
Val$_{SLP}$	DJF	-0.27	0.78	0.54	0.29	0.79	0.51	0.45	0.77	0.60	0.40[a]	0.90	0.51	0.39	0.72	0.64
	MAM	0.25	0.05[c]	0.60	0.22[a]	-0.20[a]	0.58	0.10[c]	0.08[c]	0.69	0.40[a]	-0.28[b]	0.71	0.25[a]	0.07[c]	0.63
	JJA	0.39	0.66	0.22	0.41	0.59	0.38	0.46	0.70	0.02[c]	0.58	0.36[a]	0.60	0.56	0.62	0.26[a]
	SON	-0.02[c]	0.60	0.54	0.00[c]	0.57	0.66	0.35[a]	0.70	0.51	0.55	0.65	0.24[c]	0.44	0.60	0.48
Ber$_{SLP}$	DJF	0.32	0.05[c]	0.80	-0.30	0.10[c]	0.80	-0.35[a]	-0.04[c]	0.83	-0.60	-0.01[c]	0.69	0.35	-0.15[c]	0.78
	MAM	-0.08[c]	-0.19[b]	-0.13[c]	-0.08[c]	-0.15[c]	-0.24[a]	-0.16[c]	-0.20[c]	-0.23[c]	0.01[c]	-0.01[c]	0.28[b]	0.06[c]	-0.36	-0.24[a]
	JJA	0.33	0.60	0.60	0.28	0.52	0.27	0.50	0.69	0.61	0.65	0.35[a]	0.28[b]	0.52	0.57	0.05[c]
	SON	-0.16[b]	-0.25	0.82	-0.31	-0.21[a]	0.79	-0.16[c]	-0.03[c]	0.57	0.06[c]	-0.00[c]	0.66	-0.09[c]	-0.10[c]	0.67

5

Table 5: Monthly correlations of our composite indices (EA_{comp} and SCA_{comp}) and the instrumental records (Val_{SLP} and Ber_{SLP}). (*) Spring (MAM) pattern is that of WA. See text for details. Note: all correlations with p-val≤0.01 except [a] 0.01<p-val≤0.05; [b] 0.05<p-val≤0.1; and [c] p-val>0.1.

		EA_{comp}	SCA_{comp}
Val_{SLP}	DJF	0.75	0.52
	MAM	0.65	0.05[c]*
	JJA	0.38	0.~~66~~48
	SON	0.55	0.54
Ber_{SLP}	DJF	0.03[c]	0.82
	MAM	-0.10[b]	0.08[c]*
	JJA	0.23	0.62
	SON	-0.20	0.71

5

Table 6: Monthly correlations between the CPC indices (NAO_{CPC}, EA_{CPC} and SCA_{CPC}) and our composites (NAO_{comp}, EA_{comp} and SCA_{comp}). Note: all correlations with p-val≤0.01 except [a] 0.01<p-val≤0.05; [b] 0.05<p-valv0.1; and [c] p-val>0.1. The SCA only has been compared to the composites for DJF, JJA and SON because spring is showing the WA pattern (see Table 4 and Figs. 1 and S1-S4 for further details).

10

		NAO_{CPC}	EA_{CPC}	SCA_{CPC}
Composites	DJF	0.81	-0.60	0.41
	MAM	0.64	-0.31	-
	JJA	0.79	-0.31	0.~~27~~20
	SON	0.76	-0.39	0.19

15

20

Table 7: Monthly correlations between the EA_{cpc} and SCA_{cpc} and our station-based indices (Val_{SLP} and Ber_{SLP}).
Note: all correlations with p-val≤0.01 except [a] 0.01<p-val≤0.05; [b] 0.05<p-val≤0.1; and [c] p-val>0.1.

		EA_{CPC}	SCA_{CPC}
Val_{SLP}	DJF	-0.58	-0.17[a]
	MAM	-0.47	-0.30
	JJA	-0.36	-0.01[c]
	SON	-0.54	-0.42
Ber_{SLP}	DJF	-0.26	0.32
	MAM	-0.33	0.16[a]
	JJA	-0.26	0.26
	SON	-0.38	0.24

5